The Dissertation Committee for Beth Erlichman Goldstein Certifies that this is the approved version of the following dissertation:

Single channel analysis of thiol binding to a putative site of alcohol action on the glycine receptor

Committee:

S. John Mihic, Supervisor

Richard W. Aldrich

Nigel S. Atkinson

Rueben A. Gonzales

R. Adron Harris

Single channel analysis of thiol binding to a putative site of alcohol action on the glycine receptor

by

Beth Erlichman Goldstein, B.S.

Dissertation

Presented to the Faculty of the Graduate School of

The University of Texas at Austin

in Partial Fulfillment

of the Requirements

for the Degree of

Doctor of Philosophy

The University of Texas at Austin

August, 2009

Dedication

My dissertation is dedicated to my supportive family and friends who got me through graduate school.

Acknowledgements

I would like to express my gratitude to the many people that have helped me over the years during graduate school. I would like to start by thanking my advisor, S. John Mihic, who provided me the valuable experience of working in his lab. Over the years, I had the opportunity to learn many new techniques that tested my trouble-shooting and problem solving skills that ultimately led to this dissertation research. I would like to thank John for the freedom and creativity he allowed in my research and the many discussions on lab and non-lab related matters that kept each day interesting. John was always willing to meet and provide encouraging words about my projects, making the lab an enjoyable place to work.

I would like to thank Adron Harris, Director of the Waggoner Center for Alcohol and Addiction Research, for always being available to provide extra guidance. I have enjoyed conducting my graduate work in the Waggoner Center. Since moving to UT, Rick Aldrich has been a constant help with my single channel data analysis. He was always willing to spend time explaining and clarifying concepts and help with data interpretation. I really appreciate the time he spent looking over my data and his entire lab was a wonderful resource. Along with John, Adron, and Rick, I wish to express my gratitude to the other members of my dissertation committee, Nigel Atkinson and Rueben Gonzales. My committee always listened to my ideas and provided great feedback.

The members of the Mihic lab kept every day entertaining. Rachel Phelan and Michael Roberts provided crucial help when I first joined the lab and are responsible for teaching me two-electrode voltage clamp and single channel electrophysiology, respectively. While they have moved on to other institutions, their help and insight was

crucial to my success in the lab. Recent graduate Michelle Dupre, and current lab members Lily Quan, Jelena Todorovic, Megan Tipps, and Brian Welsh were all wonderful to work with. I especially want to thank Brian, who endured hours of single channel data analysis and re-analysis with me. I can have conversations with him about the intricacies of QuB that no one else could understand and I appreciate the encouragement he provided.

I would like to thank Debbie James and Marsha Berkman for wonderful administrative support and always being quick to answer any questions.

I wish to express my sincere thanks to my parents, Marianne & Martin Erlichman, who supported my decision to attend graduate school, despite being far away from home. They have remained a constant presence in my life despite the distance. I appreciate all their Southwest flights to visit me over the years and for always offering to buy my ticket home. I also want to thank my sister, Janelle, for keeping me involved in her family's lives (Ron, Milo & Willa) despite not being able to see them day-to-day. I appreciate my family consistently visiting my home in Austin and always having a good time together.

My biggest thank you goes to my husband, Glenn, who had the good fortune of meeting me just a year into graduate school. He has always been supportive and understanding and formatting my dissertation would not have been possible without his amazing Word skills. He has an outlook on life that I constantly strive to emulate. Thank you for the consistent encouragement you have always shown me.

Finally, I would like to acknowledge the financial support that made all of this possible. NIAAA grant R01 AA11525 to S. John Mihic and various funding over the years from the NIAAA alcohol training grant (T32 AA007471 to Rueben Gonzales), the M. June and J. Virgil Waggoner Endowment, the Fred M. Jones and Homer L. Bruce Endowed Graduate Fellowships, and The University of Texas.

Single channel analysis of thiol binding to a putative site of alcohol action on the glycine receptor

Publication No._____

Beth Erlichman Goldstein, PhD

The University of Texas at Austin, 2009

Supervisor: S. John Mihic

An alcohol and anesthetic binding pocket is hypothesized to exist among transmembrane domains of the α1 glycine receptor (GlyR). Prior work has shown that amino acid residue serine-267 plays a significant role in the enhancing effects of alcohol and anesthetics and is theorized to form part of an alcohol and anesthetic binding cavity among subunit transmembrane domains. Propyl methanethiosulfonate (PMTS), an alcohol-like thiol, was previously shown to bind to a cysteine residue introduced at position 267 (S267C) and this resulted in permanent enhancement of GlyR function. If ethanol is binding to residue 267 in wildtype GlyR to potentiate receptor function then we hypothesized that covalent thiol labeling would produce receptor enhancement by the same mechanisms as ethanol. Using outside-out patch single channel electrophysiology we determined the open and closed dwell-times and burst properties of S267C GlyR in the absence and presence of PMTS. The primary consequence of PMTS binding to S267C GlyR was an increase in the lengths of burst durations, paralleling the main effect

of ethanol on wildtype GlyR. Our findings thus provide a new line of evidence suggesting that ethanol is exerting its enhancing effects on the GlyR through its interactions with amino acid residue 267 in the second transmembrane domain.

Table of Contents

List of Abbreviations xi

List of Amino Acid Abbreviations xiii

List of Figures xiv

List of Tables xv

List of Equations xvi

CHAPTER 1 | INTRODUCTION **1**

1.1 Alcohol and volatile anesthetics 1

1.2 The glycine receptor 3

1.3 Glycine binding, signal transduction, and gating 9

1.4 Allosteric modulation of the glycine receptor 10

1.5 The glycine receptor alcohol and anesthetic binding pocket 12

1.6 Glycine receptor mutations 17

1.7 The proposed structure of the alcohol binding pocket 18

1.8 Single channel kinetics 20

1.9 Dissertation aims 23

CHAPTER 2 | MATERIALS AND METHODS **25**

2.1 Mutagenesis and molecular biology 25

2.2 Chemical and solution preparation 26

2.3 Mammalian cell culture and cDNA transfection 27

2.4 Patch clamp electrophysiology 28

2.5 Single channel data analysis 30

CHAPTER 3 | PMTS LABELING OF WT AND S267C RESIDUES **35**

3.1 Introduction....35

3.2 Results....37

3.2.1 Single channel recordings of GlyR activity....37

3.2.2 The S267C mutation alters GlyR unitary conductance....39

3.2.3 Analysis of channel open dwell times....41

3.2.4 Analysis of channel closed dwell times....45

3.2.5 S267C exhibits two modes of activity in the presence of PMTS....50

3.2.6 Burst duration increases in the presence of PMTS....52

3.2.7 PMTS affects burst properties....57

3.2.8 Intraburst properties....59

3.3 Discussion....61

3.3.1 WT GlyR data in the absence and presence of PMTS....61

3.3.2 WT data compared to S267C in the absence and presence of PMTS..65

3.3.3 PMTS binding at S267C verses ethanol binding WT GlyR....68

3.3.4 Mechanistic model of the glycine receptor....73

CHAPTER 4 | CONCLUSIONS **75**

4.1 Overview....75

4.2 Alcohol and anesthetic action....76

4.3 Future experiments....78

4.4 Summary....80

Bibliography....82

Vita 89

List of Abbreviations

5-HT3	5-hydroxytryptamine, serotonin
α	alpha
ACh	acetylcholine
AChR	acetylcholine receptor
AChBP	acetylcholine-binding protein
amp	amplitude
β	beta
cDNA	complementary deoxyribonucleic acid
DNA	deoxyribonucleic acid
CNS	central nervous system
DMEM	dulbecco's modified eagle medium
EDTA	ethylenediaminetetraacetic acid
EtOH	ethanol
FBS	fetal bovine serum
GABA	gamma-aminobutyric acid
GABAR	gamma-aminobutyric acid receptor
GlyR	glycine receptor
HBSS	hank's buffered salt solution
HEK	human embryonic kidney
kHz	kilohertz
LB	luria broth
LGIC	ligand-gated ion channel
LL	log likelihood

MAC	minimum alveolar concentration
MIL	maximum interval likelihood
MTS	methanethiosulfonate
mV	millivolt
nAChR	nicotinic acetylcholine receptor
pA	picoamp
pS	picosiemens
PMTS	propyl methanethiosulfonate
P_{open} / P_o	open probability
SEM	standard error of the mean
SKM	segmental-k-means algorithm
τ	tau, time constant
τ_{crit}	critical time constant
TM	transmembrane domain
WT	wildtype
Zn^{2+}	zinc

List of Amino Acid Abbreviations

Amino acids residues are named by using a single letter abbreviation followed by the position of the residue, for example S267 means there is a serine residue at position 267. S267C implies that a cysteine residue has replaced the serine at position 267.

A	Alanine	M	Methionine
C	Cysteine	N	Asparagine
D	Aspartic acid	P	Proline
E	Glutamic acid	Q	Glutamine
F	Phenylalanine	R	Arginine
G	Glycine	S	Serine
H	Histidine	T	Threonine
I	Isoleucine	V	Valine
K	Lysine	W	Tryptophan
L	Leucine	Y	Tyrosine

List of Figures

Figure 1.1 Schematic of a single glycine receptor subunit 7

Figure 1.2 Cartoon of the glycine receptor pentamer 8

Figure 1.3 Propyl methanethiosulfonate interaction 16

Figure 3.1 Representative single channel tracings 38

Figure 3.2 The S267C mutation alters GlyR conductance 40

Figure 3.3 Representative open dwell-time histograms 42

Figure 3.4 Analysis of channel open dwell times 43

Figure 3.5 Representative closed dwell-time histograms 47

Figure 3.6 Analysis of channel closed dwell times 48

Figure 3.7 S267C exhibits low and high P_o modes in the presence of PMTS 51

Figure 3.8 Representative burst duration histograms 53

Figure 3.9 PMTS increases mean burst duration 54

Figure 3.10 Burst duration analysis 55

Figure 3.11 PMTS affects burst properties 58

Figure 3.12 PMTS affects intraburst properties 60

List of Tables

Table 3.1 Open dwell time analysis 44

Table 3.2 Closed dwell time analysis 49

Table 3.3 Burst duration analysis 56

Table 3.4 Summary table of alcohol effects on WT receptors compared to PMTS effects on S267C GlyR 72

List of Equations

Equation 2.1 Exponential probability density function……...31

Equation 2.2 Weighted mean of exponential time constants……..32

Equation 2.3 Estimation of τ_{crit}……....32

Equation 2.4 Conductance……...34

CHAPTER 1 | INTRODUCTION

1.1 Alcohol and volatile anesthetics

Humans have consumed alcoholic beverages dating back to prehistoric times. Since its discovery there has been a compulsion to drink but genetic predisposition can lead to detrimental effects of alcohol intake. Problems with alcohol afflict over 15 million adults in the United States according to the National Institute on Alcohol Abuse and Alcoholism (NIAAA). Alcoholism is a disease identified by the intense craving to drink, failure to stop drinking despite wanting to, physical dependence making alcohol a required part of your life, and tolerance resulting in consuming progressively more alcohol. Alcoholics drink despite causing irreconcilable disruptions in all areas of their lives resulting in severe health and societal consequences. The continued use of alcohol can lead to family isolation as well as liver disease, brain and organ damage and, in severe cases, death according to the NIAAA website, a resource on alcohol addiction. Alcoholism is a widespread problem for all races, genders, and nationalities. According to the World Health Organization (WHO), 140 million people in the world suffer from alcohol dependence, leading to 1.8 million deaths. Alcohol abuse has a major impact on health ranking it fifth in risk factors leading to premature death and disability. It has been estimated that for every dollar spent in developing treatments, seven dollars can be saved in health and social costs (WHO website, 2009). Despite ethanol being the most widely used depressant in the world researchers have not yet determined what genes are involved in the development of alcoholism. Counseling and medication, among other treatments, can help an alcoholic cease drinking but these methods are not always successful. In

order to create effective drug treatments and find a permanent cure for this devastating disease we need to fully understand the biological mechanisms that lead to alcoholism.

In addition to alcohol, many other drugs are misused. Drug abuse is a serious problem in the United States that results in around 40 million serious illnesses or injuries each year. Like alcohol, other addictive drugs increase dopamine levels in the nucleus accumbens. This dopamine reward pathway emerges as a common denominator in addiction (Molander and Soderpalm, 2005a). A better understanding of the molecular mechanisms of these drugs can lead to prevention of abuse.

Alcohol also functions as a general anesthetic by depressing central nervous system function. One early reported case of anesthesia use is credited to dentist William Morton who performed a surgery using diethyl ether in 1846 in front of a crowd at Massachusetts General Hospital. Anesthesia is useful in surgery because it produces unconsciousness, immobility, and amnesia, while blocking pain and is fully reversible (Urban and Bleckwenn, 2002; Miller 2005). Two classes of general anesthetics are utilized during surgery. Anesthetics administered through intravenous injection are used to induce anesthesia and then anesthesia is maintained by inhaled anesthetics. Inhalational agents first enter the lungs and from there circulate throughout the body reaching every organ including the brain by penetrating the blood brain barrier. Recovery of consciousness occurs when use has been discontinued and the concentration of anesthetic in the brain and spinal cord drops below the minimum concentrations required to maintain the various facets of anesthesia.

Volatile anesthetics, such as halothane or isoflurane, are structurally simple organic liquids that evaporate readily into vapors. The potency of volatile anesthetics is measured in terms of MAC, or minimum alveolar concentration. 1 MAC is the concentration of anesthetic in the lungs that prevents movement in 50% of people in

response to a painful stimulus (Eger et al., 1965). MAC is inversely related to potency with a low MAC indicating a higher potency drug. The MAC of a volatile substance is often inversely proportional to its lipid solubility, a relationship known as the Meyer-Overton hypothesis. In 1899, Meyer used olive oil to represent lipids, the fatty molecules in brain cells, and measured the solubility of various anesthetics. The anesthetic strength was tested in tadpoles and a correlation between solubility and potency was established. Overton (1901) found that the delivery method did not affect the positive correlation between solubility and potency. As a result of these experiments, for much of the 20th century, inhaled anesthetics and alcohol were believed to act by nonspecifically disordering or fluidizing lipid bilayers. However, several problems with lipid-based theories began to arise. The degree of disorder caused by pharmacologically relevant concentrations of ethanol (10-200 mM) in membrane lipid order can be mimicked by raising the temperature one degree (Peoples et al., 1996; Tapia et al., 1998). Experiments by Franks and Lieb (1984), using firefly luciferase, a lipid-free water soluble protein, highlighted additional problems with this theory. Despite being a lipid free enzyme the MAC/potency correlation still applied to anesthetic inhibition of firefly luciferase. There was also competition between anesthetics and the natural substrate for firefly luciferase, luciferin, demonstrating that both molecules were binding to the same site on the protein. This work led to the eventual widespread acceptance of proteins, with specific binding sites, as the molecular sites of action of anesthetics and alcohols (Franks and Lieb, 1984).

1.2 The glycine receptor

As problems with the conventional Meyer-Overton hypothesis caused it to become outdated, continuing research led to new theories of specific receptors on

neurons as sites for alcohol and anesthetic actions. This transition made ion channels a logical candidate as a primary target since they can rapidly affect neuronal activity and are widely distributed throughout the central nervous system. Voltage-activated ion channels respond to changes in the membrane potential of a neuron and stretch-activated ion channels respond to mechanical deformation of the cell membrane. Ligand-gated ion channels (LGIC) respond to the binding of a chemical messenger, which converts the presynaptic chemical signal into a postsynaptic electrical signal. This signal can trigger an action potential or halt it from propagating, mediating neuronal communication through synaptic transmission.

Experiments utilizing goats under general anesthesia demonstrated that when the spinal cord was surgically bypassed more isoflurane was required to suppress a painful stimulus and produce immobility. This suggests that receptors expressed in the spinal cord and brainstem region are involved in anesthetic-induced immobility (Antognini and Schwartz, 1993). The glycine receptor (GlyR), a LGIC, is the primary mediator of inhibitory neurotransmission in the brain stem and spinal cord and also widely distributed throughout the central nervous system (Legendre, 2001). Regions where the GlyR is predominantly expressed include: the medulla oblongata, pons, thalamus, hypothalamus, cochlear nucleus, retina, olfactory bulb, cerebral cortex and cerebellum (Betz, 1991; Ivanova et al., 2006). Molander and Söderpalm (2005b) showed that α1 GlyR subunits are expressed in the rat nucleus accumbens. This brain structure is thought to play an important role in reward and addictive behavior via the dopaminergic inputs in the mesolimbic pathway. The GlyR is also involved in the generation of motor rhythms, spinal reflex responses, and sensory signaling processing (Betz and Laube, 2006).

The GlyR, combined with gamma-aminobutyric acid ($GABA_A$ & $GABA_C$), nicotinic acetylcholine (nACh), and 5-hydroxytryptamine ($5\text{-}HT_3$) comprises the cys-loop

superfamily of LGIC (Bowery et al., 2006). This family is named for the signature loop formed by a disulfide bond between two cysteine residues located in the extracellular amino terminal domain of each protein subunit (**Figure 1.1**). The inhibitory receptors activated by GABA or glycine are anion-selective channels with predominately chloride ions flowing down their electrochemical gradients in response to agonist binding, while the excitatory receptors, nACh and 5-HT_3, are cation selective (Sine and Engel, 2006).

Structurally similar to the other receptors in this family, each α subunit of the GlyR consists of an extracellular ligand binding domain and four α-helical transmembrane (TM) domains (Pless and Lynch, 2009). An extracellular linker loop between TM 2 and TM 3 is important for signal transduction that occurs between glycine binding and channel gating (Dupre et al., 2007). In addition, there is an intracellular loop connecting TM3 and TM4. The GlyR is a pentameric complex with the subunits arranged around a central ion pore, with the TM2 from each of the five subunits contributing to the formation of this pore (**Figure 1.2;** Lynch 2004; Betz and Laube, 2006). Four α subunits (labeled 1-4) and one β subunit have been identified. The human embryonic brain stem and spinal cord are composed of α_2 GlyR subunits. In adults, this transitions to GlyR being mainly composed of α_1 subunits and, to a lesser extent, α_3 subunits. In lower vertebrates, α_4 subunits are expressed (Laube et al., 2002). The β subunit is widely expressed throughout the embryonic and adult central nervous system. Co-expression with the β subunit is required for interaction with the accessory protein gephyrin, which modifies ligand-binding properties (Maas et al., 2006). Most adult neuronal GlyR are composed of α_1 and β membrane spanning subunits. The α_1 subunit can assemble into functional homomeric receptors or $\alpha_1\beta$ heteromers, although the stoichiometry of $3\alpha_1$:2β or $2\alpha_1$:3β is disputed (Colquhoun et al., 2004; Grudzinska et al., 2005).

Glycine is the primary activating agonist of the channel while taurine acts as a partial agonist (Lape et al., 2008). Strychnine is a competitive GlyR antagonist while picrotoxin is thought to act as a chloride channel blocker. Agonists and antagonists of the GlyR share overlapping binding sites. Functionally important amino acids for glycine binding to the α1 homomeric receptor have been identified and include residues R65 and E157 (Grudzinska et al., 2005) and F159, Y161, and T204 (Laube et al., 2002). Strychnine binding requires R131 and E157 (Grudzinska et al., 2005) and G160, K200, and Y202 (Laube et al., 2002).

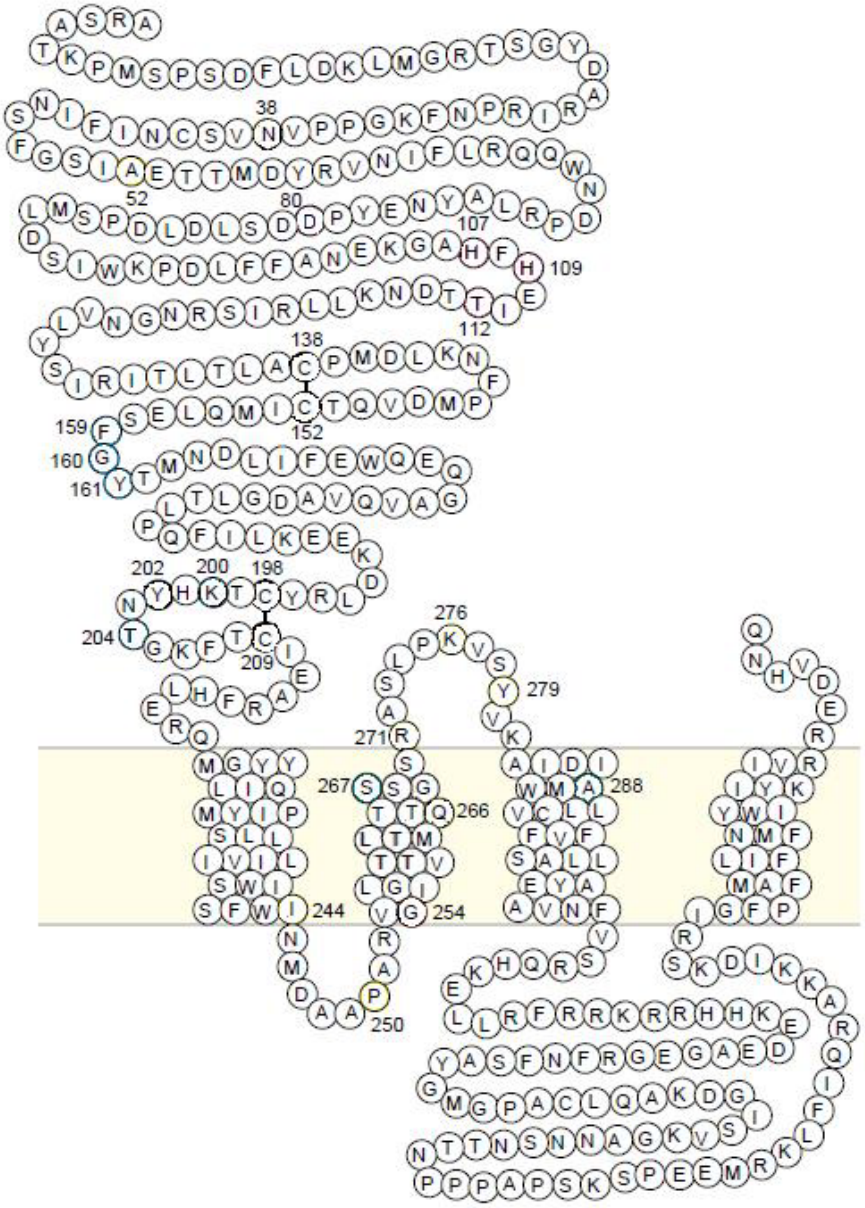

Figure 1.1 Schematic of a single glycine receptor subunit
Diagram of the amino acid composition of a GlyR subunit. The letter in each circle represents the amino acid at that position. The numbers identify the location for that specific residue. The area between the lines represents the transmembrane domain. Cysteine resides that are thought to form disulfide bonds are connected with a black line. *Adapted from Laube B, Maksay G, Schemm R, and Betz H. (2002) Modulation of glycine receptor function: a novel approach for therapeutic intervention at inhibitory synapses? Trends in Pharmacological Sciences 23: 519-527.*

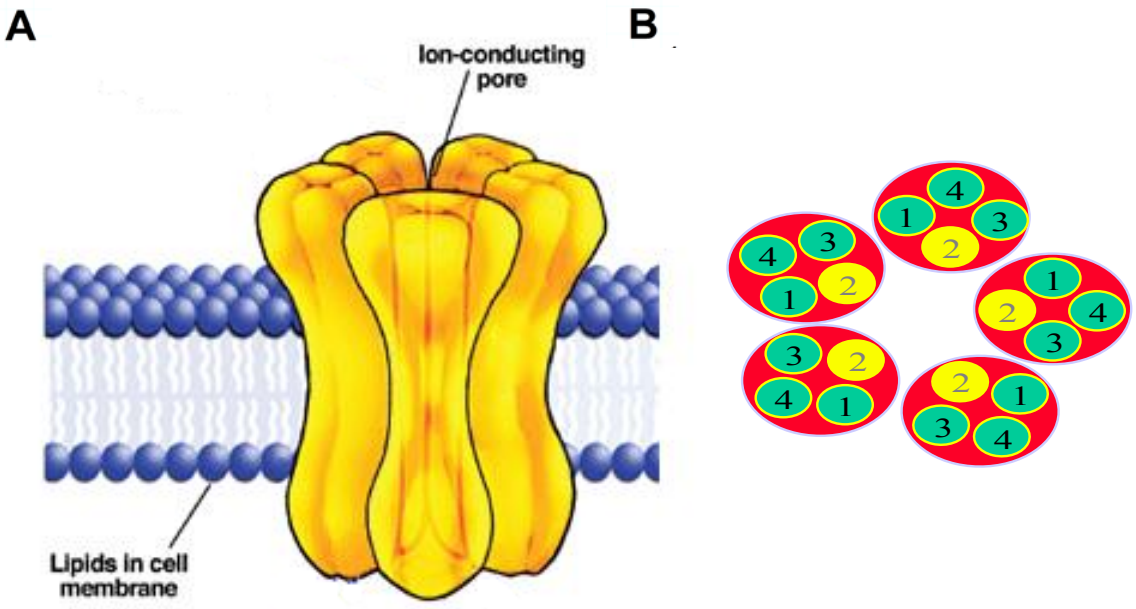

Figure 1.2 Cartoon of the glycine receptor pentamer
(A) The GlyR is a ligand-gated ion channel composed of five subunits. Agonist binding results in ion flow through the channel. *Adapted from David Lovinger. Neurons, receptors, neurotransmitters, and alcohol. Communication networks in the brain NIAAA.* (B) TM2 from each subunit of the pentamer contributes to the formation of the pore.

1.3 Glycine binding, signal transduction, and gating

Glycine binding to the GlyR causes the channel pore to open on the microsecond (μs) timescale. This allows for an influx of anions that results in fast synaptic transmission. How the signal is transduced from the ligand-binding domain to the channel pore is a complex conformational process. Using kinetic models, Beato and colleagues (2004) showed that the homomeric α_1 GlyR, which has five potential binding sites, only needed three of the five sites to be occupied for maximum gating efficacy. The ligand-binding domain of the glycine receptor is situated at the interface of neighboring subunits and composed of a β–sandwich made of inner and outer β–sheets and a series of loops. It is formed by loops A-C from the principal subunit (plus side) and loops D-F from the complementary subunit (minus side) and a coordinated interaction from both subunits is required to cause conformational transitions upon ligand binding (Pless and Lynch, 2009). The acetylcholine-binding protein (AChBP) from the snail Lymnaea stagnalis, is a useful model of the nAChR family because it has all the conserved N-terminal residues required for ligand binding although it lacks the TM domains. The crystal structure by Brejc and colleagues (2001) showed a ligand-binding pocket formed by residues from plus subunit loops and β-strands from the adjacent minus subunit. A binding cleft was seen at each subunit interface and the residues that line the cavities are implicated in nAChR ligand binding.

Unwin (2005) studied the nAChR from the muscle-derived electric organ of the *Torpedo* ray. The movement of the receptor, when agonist binds at the interface between subunits, provides a model for all cys-loop receptors. Structural analysis showed that binding caused a rearrangement of residues in the ligand-binding domain and this conformational movement transduced a signal to the transmembrane portion of the

receptor to open the gate. Subunit rotation communicates the binding signal to the TM 2-TM 3 loop, which couples binding with gating, and allows the channel to open (Unwin 2005).

1.4 Allosteric modulation of the glycine receptor

The GlyR is a target for modulation by ligands that bind at different sites than the endogenous ligand but can affect channel opening mediated by glycine. For WT receptors these allosteric modulators only produce reversible enhancement or inhibition of the response in the presence of glycine; i.e. these compounds have no effects in the absence of glycine (Laube et al., 2002). Allosteric modulators for the GlyR include alcohol, volatile anesthetics, abused inhalants, and zinc. While the alcohol, volatile anesthetics, and inhalants site of action may overlap on the GlyR (Beckstead et al., 2001), the binding site for zinc is located closer to the agonist-binding site.

Zinc, a compound found endogenously, modulates the GlyR in a biphasic manner, activating the receptor at low concentrations (~ 1 μM) and causing inhibition at higher concentrations (~ 100 μM) (Laube et al., 1995). Residues that influence zinc enhancement of the GlyR include H215, D194, E192 (Miller et al., 2005) and D80, whereas H107, H109 and T112 are involved in zinc inhibition (Laube et al., 2002). Studies show that inhibitory zinc binding occurs at the interface of adjacent GlyR α1 subunits, with H107 and H109 being found on different subunits (Nevin et al., 2003). Work by McCracken and colleagues (*submitted*) investigated the interaction of ethanol and zinc co-applied on the GlyR. Using voltage-clamped *Xenopus* oocytes they demonstrated a synergistic effect, showing that the resulting potentiation was greater then

either compound applied alone. This suggests that ethanol and zinc are interacting to modulate the GlyR.

Inhaled drugs of abuse, such as toluene and 1,1,1-trichloroethane, are also modulators of the glycine receptor and share common allosteric binding sites with alcohol and volatile anesthetics. Beckstead and colleagues (2001) showed that these allosteric modulators compete for a limited number of binding sites on the GlyR. When a volatile anesthetic was applied in combination with alcohol there was decreased enhancement compared to the compound applied alone, indicating competition for binding sites. Additionally, although a serine to isoleucine mutation at serine 267 of the α_1 subunit (S267I) renders the GlyR insensitive to ethanol, ethanol was still able to block the enhancing effects of anesthetics and inhalants when co-applied with them. This evidence indicates these compounds may have a common molecular site of action on the GlyR.

In the United States a person is considered legally intoxication with a blood alcohol concentration of 0.08% or above, which is roughly equivalent to 17mM. Low to anesthetizing concentrations of ethanol (200 mM) and 1-2 MAC concentrations of volatile anesthetics, such as enflurane and chloroform, enhance WT GlyR receptor function by binding at allosteric sites. These modulators shift the glycine concentration-response curves leftward, enhancing glycinergic current potentiation. Enhancement of GlyR function is consistent with the behavioral actions of ethanol and inhaled anesthetics observed *in vivo* at clinically relevant concentrations. Intracerebroventricular administration of glycine, or its precursor serine, enhances ethanol-induced loss of righting reflex in mice in a manner that can be blocked by the GlyR antagonist strychnine (Williams et al., 1995). Ethanol potentiates GlyR function in chick and mouse embryonic spinal neurons (Celentano et al., 1988, Aguayo and Pancetti, 1994) by decreasing the

glycine EC_{50} (Aguayo et al., 1996). No effect of ethanol is seen when it is co-applied with a maximally-effective glycine concentration. Studies using dissociated VTA neurons also demonstrate ethanol potentiation of GlyR function (Ye et al., 2001). Mascia et al. (1996) showed ethanol enhancement of homomeric α1 GlyR function using receptors expressed in *Xenopus* oocytes. Concentrations as low as 10 mM ethanol were effective, especially when lower concentrations of glycine were tested. GlyR found in the nucleus accumbens are implicated in self-administration of alcohol in Wistar rats. In vivo microdialysis of glycine increased extracellular accumbal dopamine levels and decreased ethanol consumption, while perfusion of strychnine had the opposite effect (Molander et al., 2005) In *Xenopus* oocytes volatile anesthetics at 1-2 MAC produced potentiation of glycine-gated currents (Downie et al., 1996) and subsequent experiments with rats showed strychnine infusions increased MAC for anesthetics (Zhang et al., 2003). Although the mechanisms of enhancement are not fully understood, volatile anesthetics and alcohol modulate the GlyR via similar pathways.

1.5 The glycine receptor alcohol and anesthetic binding pocket

Expanding on the idea that proteins possess binding sites for alcohol and anesthetics, Mihic and colleagues in 1997 addressed the question of what amino acids are critical for binding. Using chimaeric receptor constructs they identified a region of the GlyR essential for receptor modulation by anesthetics and alcohols. The amino acids serine at position 267 (S267) in TM2 and alanine at 288 (A288) in TM3 appeared to be specific targets for determining anesthetic and alcohol sensitivity for the GlyR. Mascia et al. (2000) further addressed this putative alcohol binding region of the GlyR by mutating the serine residue at position 267 to a cysteine (S267C), for the purpose of covalently

binding an alcohol-like thiol compound. Cysteine mutagenesis combined with a water-soluble sulfhydryl reagent that results in covalent chemical modification is a powerful technique for determining amino acid positioning (Xu and Akabas, 1993). Reacting the uncharged thiol reagent, propyl methanethiosulfonate (PMTS; Figure 1.3), with a single cysteine residue introduced in the putative alcohol binding site determined the accessibility of the cysteine since the reaction with PMTS is much faster when the residue is in a water-filled environment (Lobo et al., 2004a ; Jung et al., 2005). The reaction between PMTS and the substituted cysteine requires that the sulfhydryl side chain of the cysteine is ionized and reactive, with ionization occurring predominantly in the presence of water. In the ionized state, the cysteine and PMTS molecule can covalently react to label the cysteine. This reaction is at least 5 X 10^9 faster with an ionized –S than an unionized –SH side chain. In contrast, ionization and PMTS reactions are rare at the lipid surface and protein interior due to a low dielectric constant (Karlin and Akabas, 1998). As a result, there is no lasting effect of PMTS modulation on WT receptors and PMTS does not bind with any native cysteine residues existing in the WT GlyR. The reaction with PMTS and a cysteine residue also produces sulfinic acid and water (Dime, 1997). Covalent binding of PMTS to the S267C site irreversibly affected receptor function by enhancing glycine responses and preventing the enhancing actions of alcohols and anesthetics applied subsequently. This provided significant evidence that alcohols and anesthetics are physically interacting with amino acid 267 and suggested that this TM2/TM3 region forms a binding pocket for alcohol and inhaled anesthetics. The size of the putative 'alcohol binding pocket' was investigated in a study by Ueno et al. (2000) who showed that only amino acids on the extracellular half of TM2 are important in determining alcohol effects on $GABA_A$ receptors.

Lobo and colleagues (2004a) further investigated the role of S267 in the alcohol binding pocket by examining its water accessibility. When mutated to cysteine, S267C receptors were accessible to PMTS in the open or closed state and exhibited a permanent change in receptor function. Since MTS reagents rapidly form disulfide bonds in the presence of water, S267 must reside in the area of a water-filled pocket. No lasting effects are seen with WT receptors indicating that the MTS reagent must act at the cysteine mutation. Through a cross-linking study it was shown that S267C and A288C (in TM3) can form an intra-subunit disulfide bond and this orients the position of the residues towards a common cavity (Lobo et al., 2004b). Additionally, homology modeling revealed that these amino acids residues of the GlyR, known for their involvement in producing anesthetic effects, line a water-filled pocket among transmembrane regions where alcohols and anesthetics can bind within these channels (Bertaccini et al., 2005).

The size of the amino acid at position 267 of the GlyR also plays an important role in alcohol cutoff and modulation. Wick et al. (1998) illustrated that the replacement of the small amino acid serine at position 267 in GlyR α1 TM2 with a larger one (glutamine) decreases the alcohol cutoff, suggesting that the modified subunit possesses a smaller binding site for alcohols. The converse experiment on the GABA ρ1 subunit, replacing larger amino acid residues with smaller ones, increases its alcohol cutoff. Ye et al. (1998) demonstrated that the size of the amino acid at position 267 of the GlyR determines allosteric modulation by alcohols. There was an inverse correlation between the volume of the amino acid side chain and alcohol response, with a smaller side chain residues yielding greater potentiation.

Other amino acid residues have been identified as playing a role in the putative alcohol and anesthetic binding pocket. Crawford et al. (2007) demonstrated a balance

between negative modulation produced by alcohol at position A52 in the N-terminal domain of the α1 GlyR and positive modulation at S267. I299 in TM1 (Lobo et al., 2008) and W407, I409, Y410 and K411 in TM4 (Lobo et al., 2006) are also thought to constitute part of this pocket. It has also been postulated that the potentiating effects of ethanol on GlyR can be attributed to the TM3-4 intracellular loop and Gβγ signaling (Yevenes et al., 2008). Two motifs (316–320 and 385–386 GlyR α1 subunit) were critical for enhancement by pharmacologically relevant concentrations of ethanol (≤ 100 mM). Unlike the putative binding sites within TM domains that are shared by alcohol and volatile anesthetics, these motifs were ethanol specific and not required at higher alcohol concentrations (500 mM). This suggests the idea that low concentrations of ethanol may regulate channel function by intracellular signals while higher concentrations directly bind within the ion channel.

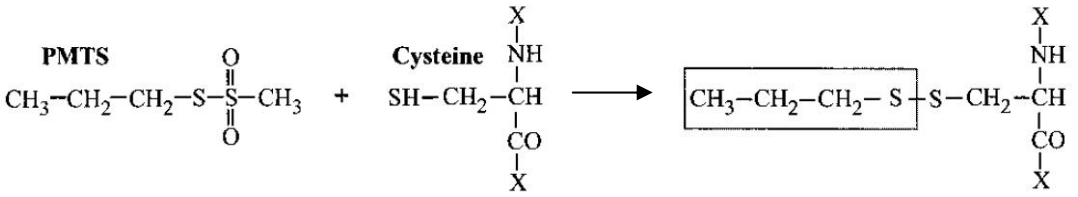

Figure 1.3 Propyl methanethiosulfonate interaction
When PMTS interacts with a cysteine residue it forms a disulfide bond. *Adapted from Mascia MP, Trudell JR, and Harris RA. (2000) Specific binding sites for alcohols and anesthetics on ligand-gated ion channels. Proc Natl Acad Sci 97(16):9305-9310.*

1.6 Glycine receptor mutations

Some mutations in the GlyR can profoundly disrupt normal function. Altering a residue, especially in a highly conserved region, can have drastic consequences. For example, hyperekplexia, characterized by a pronounced startle response, can be the result of a variety of GlyR mutations including: I244N, P250T, Q266H, R271Q/L, K276E or Y279C (Laube et al., 2002). *Spasmodic* mice exhibit a decrease in glycine sensitivity due to a missense mutation in the α1 subunit of the GlyR yielding the A52S mouse (Laube et al., 2002) while *spastic* mice show a decreased number of functional receptors due to a mutation in the β subunit. These two mutant mouse lines display altered hypnotic effects of alcohols and anesthetics and have tremors and an exaggerated startle response (Quinlan et al., 2002).

Mutating the GlyR α1 subunit amino acid from a serine to a glutamine residue at position 267 (S267Q) resulted in insensitivity to the enhancing effects of ethanol, in receptors expressed in oocytes. An *in vivo* model to evaluate GlyR function showed that S267Q transgenic mice exhibit decreased alcohol sensitivity in behavioral tests (Findlay et al., 2002). Mice with a S267Q point mutation showed an increased acoustic startle response and limb clenching. The mutation decreased GlyR efficacy and the homozygous knock-in mice exhibited seizures and died within a few weeks (Findlay et al., 2003). A GlyR subunit point mutation at the same amino acid position showed evidence for a common drug-binding site. When isoleucine replaced serine at position 267 (S267I) the effects of alcohol were abolished in an oocyte expression system. Despite having no effect itself, alcohol was still able to antagonize the actions of other drugs when co-applied. This emphasizes the specificity of certain amino acid residues in normal GlyR function (Beckstead et al., 2001).

As described above (section 1.4) Mascia et al. (2000) also showed the importance of amino acid residue S267 for alcohol and anesthetic modulation. When the cysteine that replaced the serine was covalently labeled with a thiol reagent GlyR function was irreversibly potentiated and normal binding competition with other anesthetics was lost. This conservative point mutation is very useful for studying alcohol and anesthetic modulation of the GlyR. The serine to cysteine mutation is the result of altering just one nucleotide in the GlyR α1 subunit cDNA. As a result, there should be no difference in the transcription or translation rates between WT or S267C GlyR assembly. GlyR assembly is governed by amino acids in the extracellular, N-terminal domain of the subunit, away from TM2 where S267C is located (Griffon et al., 1999). Chemically, the substitution of a cysteine residue for a serine involves exchanging a hydroxyl group for a sulfhydryl group. Additionally, the mutation does not alter the glycine concentration-response curves for homomeric or heteromeric S267C receptors, suggesting GlyR function is not markedly changed (Roberts et al., 2006).

Comparing WT GlyR function with the consequences that occur in the presence of a point mutation is a useful experimental approach to assess the function of a specific amino acid. The changes produced in GlyR channel function can help assess the role of an individual amino acid.

1.7 The proposed structure of the alcohol binding pocket

Alcohols and anesthetics are hypothesized to potentiate GlyR by binding in a water-filled cavity formed between TM2 and TM3. Homology modeling shows that amino acid residues important for alcohol and anesthetic binding line this space, forming the binding pocket (Bertaccini et al., 2005). Similarly, thiols also enhance GlyR function

by occupying space within a water-filled pocket and designing GlyR with a S267C mutation has provided evidence that this amino acid constitutes a site of physical interaction with alcohol and anesthetics (Mascia et al., 2000).Structural data for the nicotinic acetylcholine receptor, another Cys-loop family member, indicated that there is a water-filled crevice located between the transmembrane domains of each receptor subunit. A 4A° resolution atomic model of the pore domain was created using the electric organ of the Torpedo electric ray which is highly enriched in ACh-receptor-containing membranes. The S267 residue implicated in alcohol and anesthetic binding in the GlyR aligns with L257 of the AChR, which faces a cavity suitable for similar binding (Miyazawa et al., 2003).

Determining the structure of the *Drosophila* melanogaster odorant-binding protein LUSH identified a single alcohol binding site within a pocket (Kruse et al., 2003). This alcohol binding site contained a structural motif that is also seen in other alcohol sensitive ion channels including: GlyR α1, GABAR α2, AChR α, and SHAW2, the alcohol-sensitive region of the *Drosophila* voltage-sensitive potassium channel. This conserved structural motif contains a serine at position 52 in LUSH, which corresponds to S267 for the GlyR. This serine is present at the homologous position for all the alcohol sensitive receptors indicated above. This structural motif represents a commonality among alcohol binding sites and provides a high affinity-binding site for alcohol.

Without X-ray crystallography data for the GlyR there is little structural information about alcohol binding. However, the structural motif identified from the high-resolution crystal structure of butanol bound to LUSH can help predict relevant information on where alcohol is binding in the GlyR.

1.8 Single channel kinetics

In 1991 Sakmann and Neher won the Nobel Prize in physiology or medicine for developing a technique to measure electrical current that passes through a single ion channel. For the first time, this tool allowed for the observations of ion channel behavior at a single protein level. This important discovery made it possible to study the function of individual ion channels as they opened and closed (Neher and Sakmann 1976). This novel method provided the ability to form a tight seal between a cell and a glass pipette. Precautions with constructing the pipette tip led to high resistance giga-seals and improved current recordings (Hamill et al., 1981). This scientific achievement allowed extremely small currents to be recorded and analyzed and is a method that has been used extensively to study the activation mechanism of every type of ion channel including the GlyR.

In 2002, Beato and colleagues detailed the single channel activation mechanism of the α1 homomeric GlyR. Steady-state outside out patches of a single channel in the presence of low glycine (0.3, 1, or 10 μM concentrations) were used to provide an initial kinetic scheme for GlyR activation. When glycine molecules bound the main conductance level of the receptor was primarily 60 – 90 pS, with a subconductance level around 40 pS, regardless of agonist concentration. Open dwell time analysis required four exponential functions to describe the data and time constants were not agonist dependent. Burst durations were also best fit with four exponential components with an optional fifth component needed at higher glycine concentrations. The mean burst duration increased at higher glycine concentrations. The time constants remained consistent regardless of concentration but the areas of each component changed. Based on the data it seemed that a single glycine molecule binding to the GlyR causes channel opening but binding of

additional glycine molecules (higher concentrations) increased both the likelihood and duration of opening events. This lead to the idea that the number of agonist molecules bound influences what state the GlyR opens to. Because a homomeric GlyR has five agonist binding sites, a mechanistic model was created with five open states and six closed states (Beato et al., 2002). A follow up study in 2004 by Beato and colleagues modified their original mechanism of GlyR function. Single channel outside-out recordings of homomeric α1 GlyR were made in the presence of higher glycine concentrations (10 – 1000 μM). The higher glycine concentrations resulted in clusters of activity, which like bursts, are the openings resulting from the activation of a single ion channel. When the data were fit with a kinetic mechanism, it was revealed that a model with only three binding sites was needed to best describe GlyR function. Despite there being five potential binding sites, maximum gating efficacy was reached when 3 binding sites were occupied (Beato et al., 2004). A study from the same lab then fit a mechanistic model to heteromeric α1β GlyR activation. They found that the best fit also occurred when up to three binding sites were occupied and that the binding affinity increased as more glycine molecules bound (Burzomato et al., 2004). These single channel studies showed that, as the agonist concentration increased, the probability of channel opening increased, resulting in longer GlyR open dwell times. Similarly, cluster analysis showed that higher glycine concentrations resulted in longer burst durations.

Allosteric modulation of the GlyR by ethanol enhances single channel kinetics through a different mechanism than high glycine concentrations. Findings by Welsh et al. (2009) suggest that alcohol exerts its effects on the GlyR primarily by increasing the mean burst duration. At 200 mM ethanol, the number of openings per burst increased without affecting the intra-burst P_o. Unlike high concentrations of glycine there is no effect on open or closed dwell times in the presence of ethanol. Using single channel

electrophysiology Laube et al. (2000) found that zinc similarly altered α1 GlyR kinetics. At low concentrations zinc modulated the WT receptor by affecting the channel open probability with no change in conductance. The opening frequency and mean burst duration were both increased. At higher zinc concentrations the open time and burst durations were decreased compared to WT. This was due to an increase in τ2 combined with a reduction of the longest burst time constant as opposed to the increase in τ3 in the presence of low zinc. In neuronal nicotinic receptors an application of zinc (100 μm) led to an increased open probability due to increased burst duration (Hsiao et al., 2008). Neurosteroid effects on the closely related $GABA_A$ receptor were evaluated by Akk and colleagues (2004). Using single channel electrophysiology they revealed that there are multiple binding sites and steroids bind based on their structure. Increases in open time prevalence (amp_3) and duration of a longer open time (τ_3) were among the complex kinetic changes. Neurosteroids affect the open and closed time distributions of the $GABA_A$ receptor.

Experiments investigating the alcohol binding pocket location in *oocytes* have been performed at the whole cell level but single channel electrophysiology techniques are required to explore specific parameters of function of individual ion channels isolated from the cell. Outside-out patch clamping provides the opportunity to expose a membrane-bound ion channel to agonist and drugs and record the resulting current changes. This technique provides the capability to analyze conductance, open and closed dwell times, burst, and intraburst channel properties in the absence and presence of modulators, to determine what changes produce the effects of modulators seen at the whole cell level.

1.9 Dissertation aims

In this study we ask if the addition of PMTS to the S267C GlyR produces enhancement of GlyR function by a mechanism similar to that of ethanol's effects on WT GlyR. PMTS was selected since it mimics a small alcohol in size but can permanently bind to an introduced cysteine residue in the S267C GlyR mutant. This enables us to test the hypothesis that the enhancing effects of ethanol and volatile anesthetics are due to the addition of volume within the TM2-TM3 binding pocket. We would predict that if ethanol acts at this site then the consequences of thiol binding at S267C should mimic the effects produced by ethanol on WT GlyR. Using the technique of single channel electrophysiology we determine conductance, open and closed dwell times, and burst properties in the presence and absence of PMTS. We conclude that PMTS enhances GlyR function by a manner similar to that of ethanol, providing a new line of evidence that this amino acid residue in TM2 binds alcohols and anesthetics.

The aims of this dissertation are to characterize WT GlyR and study how a mutation at the putative alcohol binding site affects potentiation by an alcohol analog and compare the results to those produced by ethanol. Two aims were explored:

Aim 1: To determine the conductance and single channel open and closed dwell time properties of WT and S267C glycine receptors in the absence and presence of PMTS.

Aim 2: To determine the burst and intraburst properties of WT and S267C glycine receptors in the absence and presence of PMTS at the single channel level.

This project is divided into two aims because Aim 1 deals with the overall sequence of events in a recording including every opening and closing event. Aim 1 measures how the receptor switches between open and closed events. Aim 2 divides the data into activations of individual channels. However, both aims study the behavior of the GlyR so they are included in the same chapter.

CHAPTER 2 | MATERIALS AND METHODS

2.1 Mutagenesis and molecular biology

Human WT α1 GlyR cDNA was previously subcloned into the pBK-CMV expression vector modified by the removal of the *lac* promoter and the *lacZ* start codon (Mihic et al., 1997). The construct was transformed into XL1-Blue supercompetent *E. coli* cells (Stratagene, La Jolla, CA) and streaked on LB agar plates containing 50 μg/ml Kanamycin. Only successfully transformed colonies grew due to the Kanamycin resistant pBK-CMV vector. Colonies were selected and grown overnight in liquid LB cultures in a shaking incubator. GlyR cDNA was isolated using the HiSpeed Plasmid Maxi Kit following the protocol provided (Qiagen, Valencia, CA). cDNA concentrations (μg/μl) and quality (A_{260}/A_{280} ratio near 1.8) were verified on a NanoDrop spectrophotometer (Thermo Scientific, Wilmington, DE).

The Quick Change Mutagenesis kit (Stratagene) was used to create a point mutation in the α1 GlyR subunit cDNA sequence, replacing a serine with a cysteine at position 267 (Mascia et al., 2000). Custom sense and anti-sense primers (Integrated DNA Technologies) that contained the correct point mutation were combined with the template α1 GlyR cDNA construct and DNA polymerase and run through a thermocycling protocol. The reaction product was digested with the *DpnI* restriction enzyme to remove the original methylated template cDNA and leave the newly-formed mutated cDNA. XL1-Blue supercompetent *E. coli* cells were transfected with the S267C cDNA as described above. To verify that the point mutation was incorporated into the cDNA constructs, samples were sent for sequencing using a dideoxy flurophore method.

Constructs containing the confirmed point mutation were then available for use with our expression systems. Human WT and S267C α1 GlyR subunit cDNA stocks are preserved in our lab.

2.2 Chemical and solution preparation

All reagents used in electrophysiological studies were purchased from Sigma-Aldrich (St. Louis, MO), except PMTS, which was obtained from Toronto Research Chemicals (Toronto, ON). All solutions used deionized and filtered water.

Internal solution was composed of: 145 mM CsCl, 10 mM HEPES, 10 mM EGTA, 2 mM $CaCl_2$, and 2 mM $MgCl_2$, at pH 7.3 with CsOH and an osmolality of ~310 mmol/kg. External solution contained: 140 mM NaCl, 5 mM KCl, 2 mM $CaCl_2$, 1 mM $MgCl_2$, 10 mM HEPES, 15 mM glucose, and 20 mM sucrose at pH 7.4 using NaOH and an osmolality of ~325 mmol/kg.

Glycine was prepared by making a 10 mM stock; 37.5 mg of glycine added to 50 ml of external solution in a 50 ml polypropylene conical tube (Falcon) and vortexed until the chemical went into solution. 10μM glycine was prepared by adding 50 μl of glycine stock to 50 ml external solution.

To prepare 10 μM glycine with 5 mM PMTS, 20 μl glycine (taken from stock) was combined with 15.4 μl PMTS in 20 ml external solution. For bound PMTS experiments a 300 mM PMTS stock solution was made by adding 2.31 μl PMTS into 47.69 μl dimethyl sulfoxide. This was made on ice in the fume hood and stored in the freezer. For 50 μM PMTS, 2.5 μl of PMTS stock solution was diluted in 15 ml external solution.

2.3 Mammalian cell culture and cDNA transfection

All experiments were performed using human embryonic kidney (HEK) 293 cells (American Type Culture Collection, Manassas, VA) and grown according to standard cell culture techniques (Freshney, 2000). The cells were incubated in a 5% CO_2 / 95% O_2 atmosphere at 37C and cultured in 90% DMEM plus L-glutamine and sodium pyruvate (Invitrogen, Carlsbad, CA), supplemented with 10% fetal bovine serum (Gemini Bio-Products, West Sacramento, CA). Cells were grown in 10 cm round, cell culture-treated plastic Petri dishes (Corning Life Sciences) and split every two to three days to maintain an 80% confluency. To split, cells were treated with 0.25% trypsin and 1 mM EDTA in HBSS (Invitrogen), which caused the cells to detach from the Petri dish. Aliquots were put into new petri dishes with DMEM + FBS and were ready for experimental use around passage 3. Cell cultures were maintained through passage 15, when a new aliquot of cells was started.

An optimized protocol using PolyFect transfection reagent (Qiagen) was used to transiently transfect the cells with WT or mutant α1 GlyR cDNA on 15 mm Nunc Thermanox coverslips (Cole-Parmer, Vernon Hills, Il) in 6-well plates. The PolyFect reagent is an activated-dendrimer that forms a complex with the plasmid DNA and is readily taken up into the cells (Tang et al., 1996). Once inside the DNA can be transcribed into mRNA and then translated into GlyR subunits. To keep the GlyR expression level low, which is useful for single channel recordings, the transfection mixture contained only 5 - 10% α1 GlyR cDNA and was combined with empty pBK-CMV vector (Groot-Kormelink et al., 2002). cDNA of CD4, a cell surface marker, was co-transfected and anti-CD4 Dynabeads (Dynal Biotech, Oslo, Norway) were used to determine which cells to test for GlyR expression.

A mixture containing 0.08 μg GlyR cDNA, 0.15 μg CD4 cDNA, 1.4 μg pBK-CMV empty vector cDNA, and 10 μl of PolyFect reagent was prepared for each transfection and incubated for 10 min at room temperature before being applied to the cells. After six hours in the incubator the transfected cells were washed and ready for experimental use.

2.4 Patch clamp electrophysiology

Patch clamp electrophysiology experiments were conducted 1-5 days after transfection to ensure optimal expression levels. Outside-out patches were pulled and current recordings made following standard techniques (Hamill et al., 1981; Sakmann and Neher, 1995). Patch pipettes were pulled from thick-walled borosilicate glass (World Precision Instruments, Sarasota, FL) using a P-97 Flaming/Brown micropipette puller (Sutter Instruments). The glass had an outer diameter of 1.5 mm and an inner diameter of 0.75 mm. Next, the barrel region just above the electrode tip was coated with Sylgard 184, a silicone elastomer that limits the formation of capacitance transients across the surface of the recording pipette (Dow Corning, Midland, MI). Finally, the tip was fire-polished with a microforge (Narishige) to form a smooth surface. These steps lead to a patch pipette that could form a tight gigaseal with the cell membrane. Establishing gigaohm (GΩ) resistance to the current flow is crucial for establishing a high signal to noise ratio for detection of activity in single channel recordings.

Experiments were performed using the outside-out patch configuration which first required obtaining a cell-attached patch. This was achieved by lowering the patch pipette until it pressed against the cell membrane and lightly applying suction to form a gigaseal. Next, a whole-cell configuration was formed by applying additional suction to break into

the membrane. Lifting the pipette up and away from the cell detached a patch of membrane resulting in outside-out configuration. The cell membrane is able to reform across the pipette tip so that the extracellular face is still exposed to the bath and the intracellular portion is exposed to the interior of the pipette. This configuration enabled us to bath apply drugs of interest while measuring currents.

The pipette was filled with internal solution and cells were continuously bathed in external solution by gravity flow from a 50 ml glass syringe. These solutions have isotonic chloride so the chloride reversal potential (E_{Cl}) for the cell is at ~ 0 mv, with an uncorrected junction potential of < 5 mV.

Agonist and drug solutions were also prepared in external solution and perfused over outside-out patches using the SF-77B Perfusion Fast Step apparatus (Warner Instruments). 20 ml glass syringes were filled with solutions and connected through polyethylene tubing to one of two manifolds. Each manifold had three inputs but only one output, allowing only one solution to flow at a time. The outputs were connected to a pulled theta glass capillary. Patches were positioned directly in front of the theta glass capillary in the recording chamber and solutions were delivered through gravity flow. A solution was always flowing through the glass outlets during experiments and the theta glass allowed for rapid solution exchange if necessary (ms time scale).

Single channel recordings were made under steady state conditions. External solution was bath applied during setup and then switched to glycine (10 μM) or glycine plus PMTS perfusion for the duration of the experiment. For experiments using WT transfected cells, PMTS was prepared to a final concentration of 5 mM in external solution and continuously co-applied with glycine. For experiments using S267C transfected cells, PMTS was prepared to a final concentration of 50 μM in external solution and applied once for 60 seconds to the entire coverslip in a small Petri dish; a

lower PMTS concentration was used with the S267C mutant because it can bind PMTS permanently. After washing unbound PMTS from the coverslip with external solution the coverslip was transferred to the bath for electrophysiological studies.

2.5 Single channel data analysis

Single channel data were acquired with pClamp version 9 software using an Axopatch 200B amplifier (Axon Instruments, Union City, CA). The amplifier reduces noise in two ways. First, it uses a capacitor-feedback integrating headstage that converts current signals entering through the recording electrode into voltages with minimal noise pickup. Second, the headstage is cooled to –15 C by a Peltier device. Recordings can be made at 10 kHz using this circuitry with a root mean square noise of < 145 femtoAmps. Outside-out patches considered for recordings needed a seal resistance > 10 GΩ. This was determined by generating a 5 mV voltage step and seeing what magnitude of current was required. Patches were all voltage clamped at –60 mV. The analog output of the Axopatch 200B voltage clamp was filtered at 10 kHz through a 4-pole lowpass Bessel filter. Data were digitized at 50 kHz through a Digidata 1322 (Axon Instruments) and stored on a computer hard drive for later analysis. The Clampex program permitted electronic control over the clamped membrane voltage, the data-sampling rate, and the perfusion motor.

Tracings were exported from ClampEx and data files were cleaned up using the single channel analysis programs in QuB version 1.4.0.125 created in the laboratory of Anthony Auerbach at State University of New York at Buffalo (Qin et al., 1996; Qin et al., 1997; Qin et al., 2000a; Qin et al., 2000b). High-resolution recordings were pre-processed to delete noise and rare double openings that would interfere with analysis, and

baseline drift and DC offset were corrected. A clean version of the data file was extracted. A selection list of openings was made and an amplitude histogram was curve fit to determine the mean open and closed amplitudes and corresponding standard deviations. These representative current values were assigned to a simple model of a single closed state connected to a single open state.

The data file, using a deadtime of 60 μs, was idealized using segmental-k-means (SKM), a hidden Markov algorithm, which detected opening events (Qin, 2004). The idealized data file is a list of opening and closing durations in the order they occurred. Channel open dwell times were analyzed using the maximum interval likelihood (MIL) algorithm. The probability density function below was used to fit open dwell time histograms with a single exponential or the sum of multiple exponentials. Amp (a_i) is the percent likelihood that a channel will open to a particular component corresponding to tau (τ_i), the time constant of the component.

$$f(t) = \sum a_i \tau_i^{-1} e^{-t/\tau_i} \qquad \textbf{\textit{Equation 2.1}}$$

Closed dwell time histograms were also fit using MIL. Histograms were fit initially with a single exponential represented by a model with one closed state connected to one open state (C→O). To provide a better fit of the data additional exponentials were added. This iterative process corresponded to building a star model by adding open and closed states alternately to the original center closed state. The MIL algorithm was run after every component addition. Changes in log likelihood (LL) values, a measure of fit quality, roughly determined if the additional state was necessary and was confirmed by visual inspection of histogram fits of the data.

Once the data was best fit with the appropriate number of exponential components corresponding to the number of states in the star model, the data were re-idealized to obtain a final histogram fit and model rate estimates. For each exponential curve required, τ_i and a_i values were provided by MIL for dwell time analysis. a_i is the percentage of data described by that particular component and τ_i is the time constant of the component. Channel mean open time was calculated by measuring the open lifetime of every opening event and diving by the total number of open events. The mean open time is equal to a weighted average of the time constants according to the following function:

$$mean = \sum a_i \tau_i \qquad \textbf{Equation 2.2}$$

Data was next chopped into bursts of openings. Bursts began with an opening event from a single receptor where the ligand initially bound the receptor and terminated when the ligand dissociated and the receptor closed or the receptor desensitized. Closing events longer then a critical time (τ_{crit}) were detected and QuB calculated an individual τ_{crit} value for each patch using the following equation:

$$Amp_1 \times e^{-\tau_{crit}/\tau 1} = Amp_2 \times \left(1 - e^{-\tau_{crit}/\tau 2}\right) \qquad \textbf{Equation 2.3}$$

This equation solves for τ_{crit} by identifying the closed components that fall within bursts (intraburst) and those outside bursts (interburst) and minimizes the area under each tail that is misclassified (Colquhoun and Sigworth, 1995). In this equation amp_1 and τ_1 refer to the faster closed state component and amp_2 and τ_2 are the slower closed state component that overlap. Closed dwell time histograms for WT GlyR show a distinct

valley between exponentials where τ_{crit} falls. QuB chopped the data into burst segments leaving closings shorter then τ_{crit} within bursts and removing closings that are longer then τ_{crit} (burst termination), providing a list of burst durations.

Burst duration analysis was conducted in a similar way to open dwell time analysis. A data file of burst lengths was created from chopping the data into bursts using a unique τ_{crit} for each patch. A histogram of burst durations was fit with the exponential probability density function (**Equation 2.1**) using MIL. A star model was created to estimate the rate constants. The model initially contained a single center-closed state and only open states were added as needed based on LL values and visual inspection of fit. The burst duration histogram was best fit with 3 or 4 exponentials components depending on the condition. Tau and amp values were obtained from MIL based on histogram fits of burst duration data. Mean burst duration was calculated as the weighted average of burst duration component time constants (**Equation 2.2**).

As part of the intraburst data analysis the average number of opening events per burst was determined for each patch by dividing the number of opening events by the number of bursts. The weighted channel open probability (P_{open}) within bursts was calculated by dividing the total open time in a patch by the sum of burst lengths. This weights the data so bursts with longer durations contribute more to the P_{open} (Burzomato et al., 2004).

Conductance was calculated for each patch. Typical open events throughout the recording were selected along with baseline on either side for reference. These channel opening and closing events were curve fit using the sum of two Gaussian functions; one to fit the open current and one to fit baseline current. Some patches also showed a sub-conductance and required three Gaussian functions to fit the main, sub, and baseline

current levels properly. Conductance was calculated as the difference between the open current level and baseline, according to Ohm's law:

$$g = I / V \qquad \textbf{\textit{Equation 2.4}}$$

where g represents the unitary channel conductance, I represents the absolute current measured in picoamps (pA) for each patch, and V represents the absolute difference in membrane potential and E_{Cl} (60 mV).

All of the above analyses were conducted on individual patches (3-7 per condition) with the results averaged to calculate an overall mean value and standard error for each treatment group.

Statistical analyses were performed using SigmaStat (SPSS Inc., Chicago, IL). We compared WT GlyR in the absence and presence of PMTS using a Student's *t*-test for each single channel parameter analyzed with $p \leq 0.05$ considered significant. We also compared WT to S267C and S267C to S267C in the presence of PMTS using a one-way ANOVA to perform the statistical analysis.

CHAPTER 3 | PMTS LABELING OF WT AND S267C RESIDUES

3.1 Introduction

Alcohol is a widely abused drug and excessive use can lead to a debilitating addiction. Despite part of the population being predisposed to this disease the molecular mechanism of action is not fully understood. Being able to pinpoint the genes and the cellular targets responsible for alcoholism are important steps toward rational medical treatment. One possible target of study is the GlyR. The mechanism of alcohol action on the GlyR has recently been elucidated (Welsh et al., 2009), but where the alcohol binding pocket is formed on the GlyR remains elusive. Alcohol and anesthetics are known to both modulate the GlyR and are believed to have overlapping binding sites (Beckstead et al., 2001).

The use of anesthesia constitutes one of the cornerstones of modern medical practice. Despite its widespread use the molecular mechanism of action of anesthetics has not been conclusively determined. Research has shown that the GlyR is a specific target for volatile anesthetics (Grasshoff and Antkowiak, 2006) and that the S267 residue in TM2 likely plays a direct role in the anesthetic binding pocket (Ahrens et al., 2008).

The above cited studies and many other research efforts have shown alcohol and inhaled anesthetics affect GlyR function and that these effects are abolished when the receptor is mutated at specific amino acids. However, there is still the issue of whether these transmembrane amino acid residues actually constitute part of an alcohol ‘binding site’ or are instead responsible for transducing a signal through the receptor complex after the alcohol or anesthetic molecule interacts with the receptor elsewhere.

Work by Masia et al. (2000) using thiol binding presented the most conclusive evidence for the location of the ethanol binding site on the GlyR. These experiments utilized prior work (Mihic et al., 1997) showing that amino acid residue S267 was crucial for alcohol modulation of the GlyR. To determine if this residue was part of the putative binding pocket a S267C GlyR mutant was created. This allowed PMTS, an alcohol analog that forms a covalent bond with the sulfhydryl group of a cysteine residue, to be used in a novel way by binding it at the proposed alcohol binding location. WT GlyR potentiation by PMTS was reversible; however S267C GlyR function was permanently enhanced even after PMTS washout during *Xenopus* oocyte recordings. In addition, after PMTS application the effects of enflurane, isoflurane, and octanol were abolished on S267C GlyR despite their potentiating effects prior to PMTS application.

In our study, we took the idea one step further in a novel direction by combining the use of a thiol reagent with single channel electrophysiology. Using a compound that can bind covalently, such as PMTS, gives one the ability to control where the alcohol analog is binding to the GlyR. By creating a mutant GlyR to be compared to WT GlyR we could ensure that any changes in GlyR function observed after PMTS application were due to permanent PMTS binding at that known molecular site. We asked if the addition of PMTS to the S267C GlyR produces enhancement of GlyR function by a mechanism similar to that of ethanol's effects on WT GlyR. Using the technique of single channel electrophysiology we determined conductance, open and closed dwell times, and burst properties in the presence and absence of PMTS. These findings were then compared to those obtained in a previous study ong ethanol enhancement of the WT GlyR (Welsh et al., 2009). We found similarities in many channel parameters between the effects of PMTS covalently bound to the S267C residue and ethanol effects on WT GlyR. We conclude that PMTS enhances GlyR function by a manner similar to that of

ethanol and inhaled anesthetics, providing a new line of evidence that this amino acid residue in TM2 constitutes part of a binding site for alcohols and anesthetics.

3.2 Results

3.2.1 SINGLE CHANNEL RECORDINGS OF GLYR ACTIVITY

In this study we used single channel electrophysiology to characterize WT and the S267C α1 GlyR mutation in the presence and absence of PMTS. **Figure 3.1** shows sample tracings of outside-out patches obtained from WT and S267C α1 GlyR expressed in HEK 293 cells. An application of 10 μM glycine on WT receptors results in bursts comprised of single opening events as well as bursts containing multiple openings. In the presence of 5 mM PMTS, WT tracings exhibit fewer single events and longer burst activity. S267C channel activity in the presence of 10 μM glycine is similar to WT, with single opening events and short bursts evident. With the addition of bound PMTS, S267C burst events appear longer and occur more frequently.

Patches were voltage-clamped at –60 mV and channel openings were recorded as inward currents, indicated by downward openings. A rapid perfusion device was used to create a steady-state environment for the cell by continuously perfusing the patch with the solution being tested during the entire recording. A 10 μM glycine concentration was chosen for several reasons. A low glycine concentration was needed to minimize the occurrence of double openings and to see robust effects of PMTS modulation while still generating enough channel activity for kinetic analysis. The S267C mutation causes a decrease in the maximal current produced (Roberts et al., 2006) so a slightly higher glycine concentration was used compared to the ethanol WT study (Welsh et al., 2009).

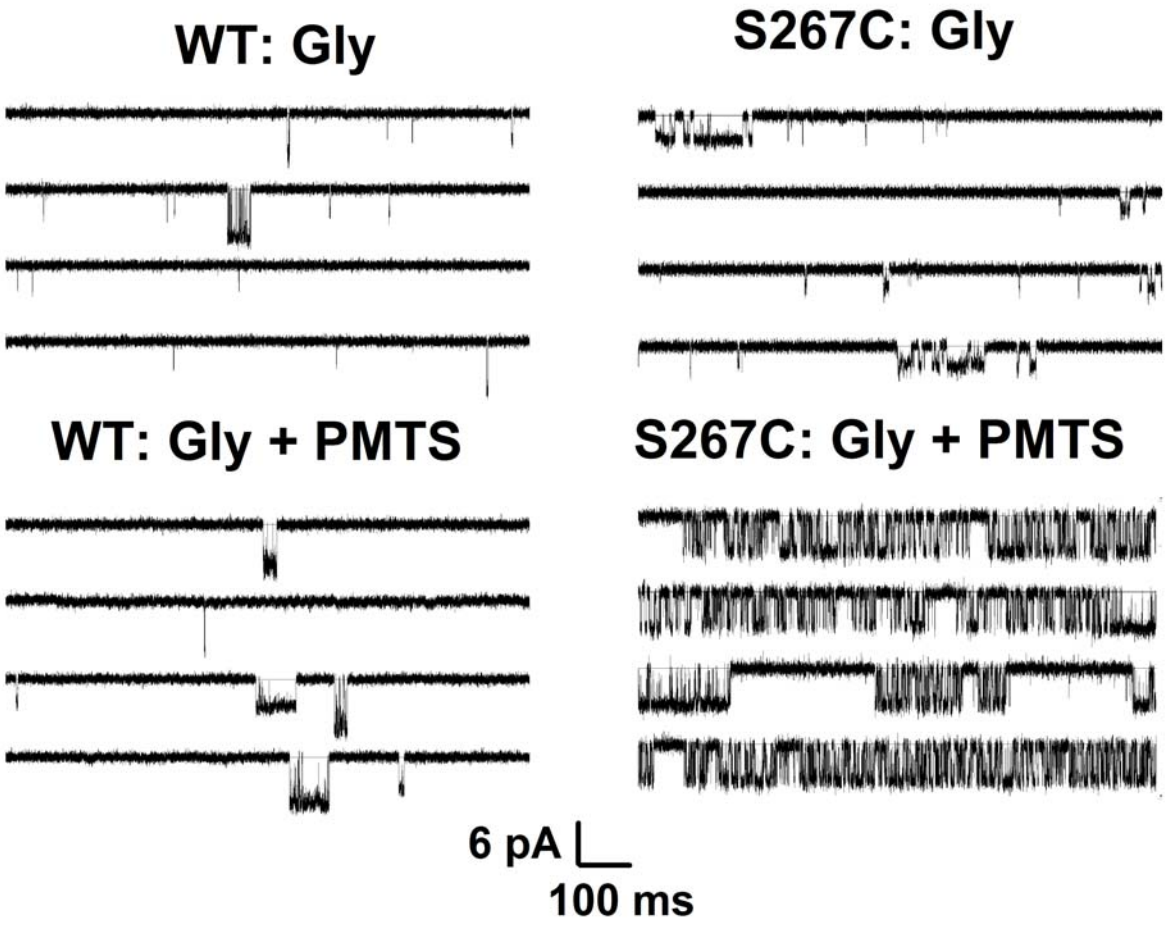

Figure 3.1 Representative single channel tracings
Homomeric α1 GlyR patches were voltage-clamped at - 60 mV and continuously perfused. WT α1 GlyR response to 10 μM glycine (top left), WT in the presence of glycine + 5 mM PMTS (bottom left), S267C GlyR response to 10 μM glycine (top right) and S267C GlyR response to glycine + bound PMTS (bottom right). Data were lowpass filtered at 10 kHz and sampled at 50 kHz. Tracings are shown digitally filtered at 3 kHz to improve visualization.

3.2.2 THE S267C MUTATION ALTERS GLYR UNITARY CONDUCTANCE

Amplitude histograms were created by selecting clusters that represented full openings, binning the data, and curve fitting the current amplitudes. The histograms were fit with two (and occasionally three) Gaussian curves. One Gaussian curve fit the open state current level and another described the closed baseline state. Since the baseline was at 0 pA after DC correction, the absolute difference between the two peaks represented the current flowing through a single channel. This was converted from open amplitude current (A) to conductance (S) by dividing by - 0.06 V, based on Ohm's law. If a third Gaussian curve was required, it fit the subconductance state.

Although similar to WT GlyR in many ways the S267C mutation did alter the conductance as shown in **Figure 3.2**. In the presence of glycine, the WT conductance did not change with the addition of PMTS [$t(6) = 0.24$, $p > 0.8$] and exhibited the same chord conductance as the S267C + PMTS group, approximately 100 pS. However, the S267C mutant tested in the absence of PMTS showed a significantly lowered conductance of 60 pS [$F(2,16) = 41.84$, $p < 0.001$] compared to WT and S267C plus PMTS. WT patches in the absence and presence of PMTS and S267C in the presence of PMTS exhibited a subconductance state that predominated in the S267C recordings as the main conductance, while the S267C in the absence of PMTS showed rare full conductance openings that predominated in the other experimental conditions. The mean chord conductance for the S267C mutant differed significantly from WT and the addition of bound PMTS to S267C GlyR restored the primary conductance level to that of WT receptors.

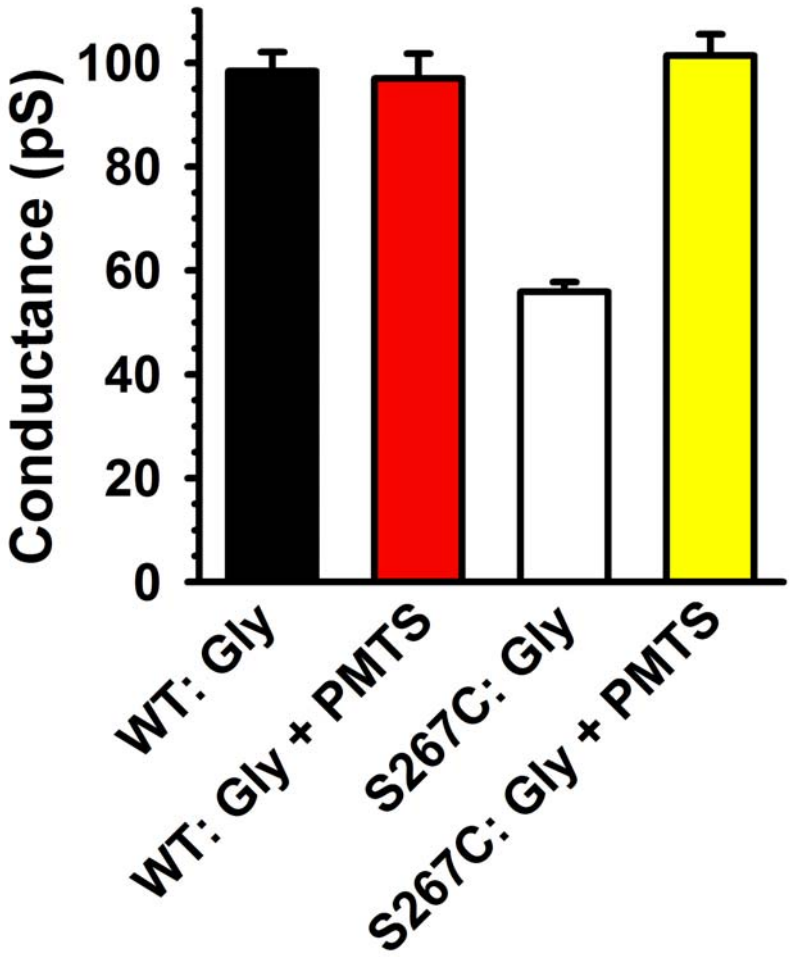

Figure 3.2 The S267C mutation alters GlyR conductance

Main conductance in the presence of 10 μM glycine was approximately 100 pS for WT GlyR, WT + 5 mM PMTS, and S267C with PMTS bound. The S267C mutant in the absence of PMTS displayed a significantly lower conductance according to a two way ANOVA. Numerous openings from each patch were binned together and fit with Gaussian fuctions. The difference between these functions was used to calculate the individual patch conductance. The conductance from all the patches for an experimental condition were averaged together to determine the overall main conductance. Data represent the mean ± S.E.M. obtained from 3 – 7 patches.

3.2.3 ANALYSIS OF CHANNEL OPEN DWELL TIMES

Single channel recordings were idealized using the SKM algorithm. Open dwell times for each experimental condition were binned according to duration and the histograms were fit with three exponential functions using the MIL algorithm (**Figure 3.3**). There were no significant effects of PMTS on the lifetimes of the three open states compared to the WT GlyR [τ_1, $t(6) = 0.58$, $p > 0.6$; τ_2, $t(6) = 0.90$, $p > 0.4$; τ_3, $t(6) = 0.62$, $p > 0.6$]. Mutation to S267C decreased lifetimes for the two shortest open times [τ_1, $F(2,16) = 9.92$, $p < 0.002$; τ_2, $F(2, 16) = 10.96$, $p < 0.001$] but not the third, compared to WT with glycine. There were no significant effects of PMTS on the lifetimes of the three open taus in the S267C GlyR (**Figure 3.4 A**).

The likelihoods (amp 1-3) of entering the shortest, middle or longest-lived open times did not depend on PMTS for WT [a_1, $t(6) = 1.09$, $p > 0.3$; a_2, $t(6) = 0.79$, $p > 0.5$; a_3, $t(6) = 1.43$, $p > 0.2$]. There was also no change in likelihood between the WT and S267C receptors. However, PMTS did increase the likelihood of observing the longest-lived open component in the S267C GlyR [$F(2,16) = 4.15$, $p < 0.04$] (**Figure 3.4 B**).

The mean open times were unchanged in WT with the addition of PMTS [$t(6) = 0.71$, $p > 0.5$] (**Figure 3.4 C**). The mean open time of WT compared to S267C with and without PMTS varied significantly [$F(2,16) = 6.75$, $p < 0.01$]. This difference could be ascribed solely to differences in the mean open times between WT and S267C GlyR, while PMTS had no significant effects on mean open time. Mean open times were significantly shorter in the S267C mutant experimental group.

These results suggest that PMTS does not exert its effect on the GlyR by stabilizing the open state (**Table 3.1**).

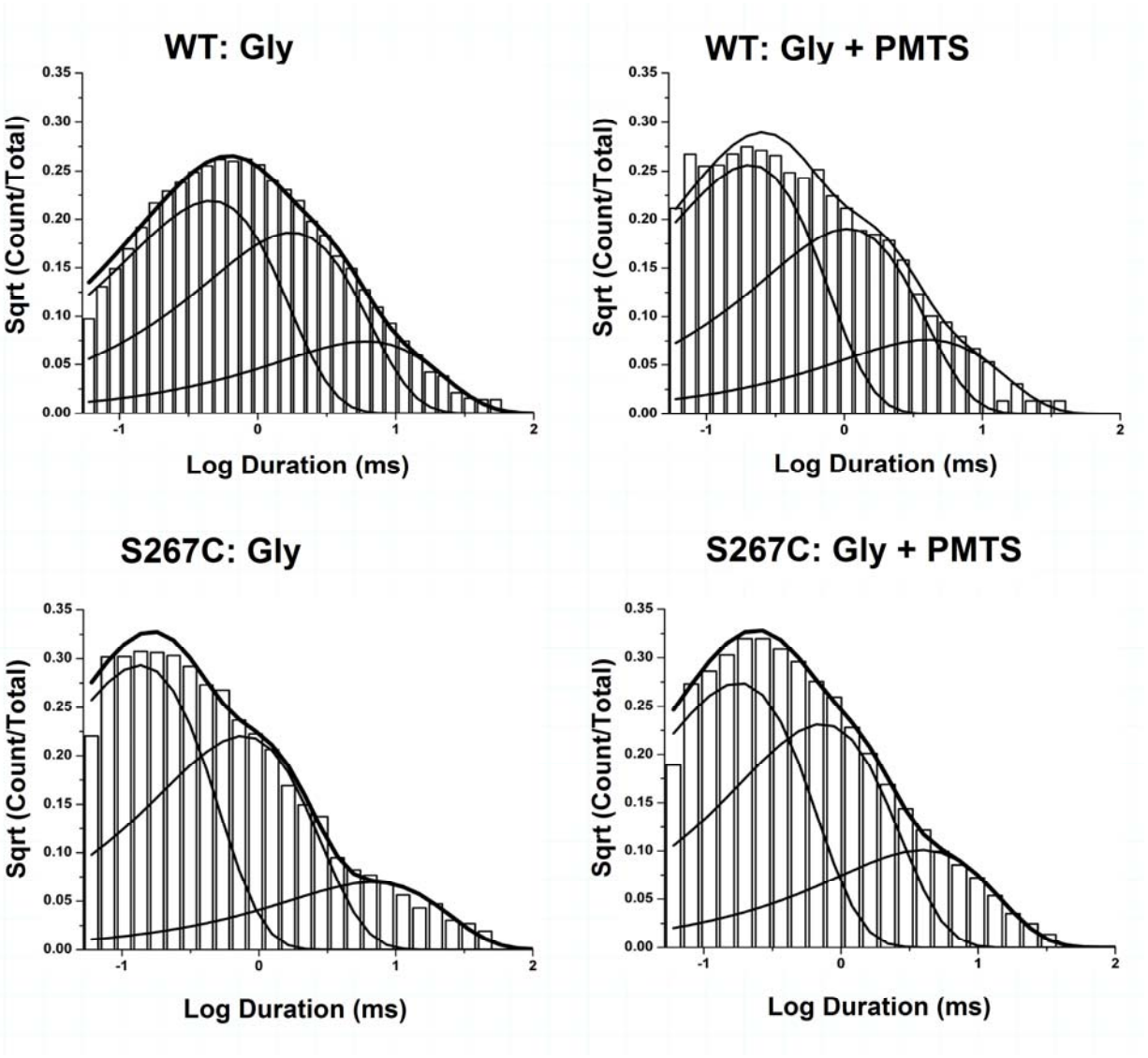

Figure 3.3 Representative open dwell-time histograms
Each condition was fit using three open time components (τs). The top line is an overall fit of all the data while the other lines describe the individual open dwell-time exponential functions. The ordinates are on a log 10 scale and the abscissas are on a square root scale in order to show the range of dwell times more clearly.

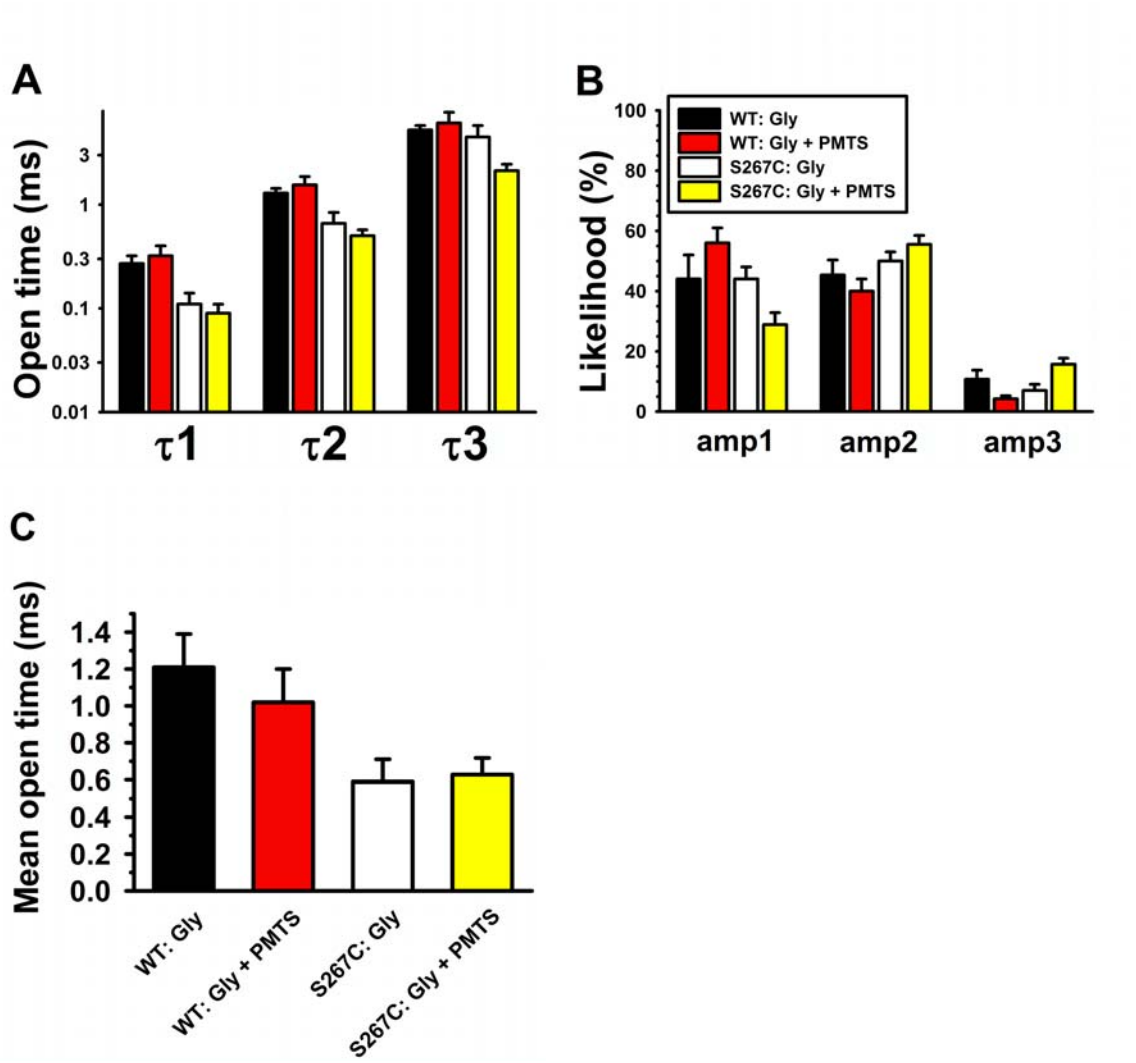

Figure 3.4 Analysis of channel open dwell times
(A) Mutation to S267C decreased lifetimes for the two shortest open times but not the third. Addition of PMTS had no significant effects on WT or S267C open dwell time components. (B) The likelihood of opening to a particular open time component did not differ between WT and S267C but addition of PMTS did increase the likelihood of entering the longest-lived open component in the S267C GlyR. (C) The S267C GlyR mutation produced a decrease in mean open time compared to WT GlyR that was not affected by PMTS binding on WT or S267C. Data represent the mean ± S.E.M. obtained from 3 – 7 patches.

Table 3.1 Open dwell time analysis

	n (events)	τ_1 (ms)	a_1 (%)	τ_2 (ms)	a_2 (%)	τ_3 (ms)	a_3 (%)	Mean Open Time (ms)
WT	113,171	0.27 ± 0.05	44.0 ± 7.6	1.29 ± 0.14	45.3 ± 4.7	5.24 ± 0.55	10.7 ± 3.3	1.21 ± 0.18
WT PMTS	40,309	0.32 ± 0.08	55.9 ± 4.5	1.55 ± 0.31	39.9 ± 3.9	6.11 ± 1.63	4.2 ± 1.3	1.02 ± 0.18
S267C	64,255	0.11 ± 0.03	43.7 ± 4.1	0.66 ± 0.18	49.5 ± 2.8	4.48 ± 1.31	6.8 ± 1.5	0.59 ± 0.12
S267C PMTS	364,961	0.09 ± 0.02	28.8 ± 4.0	0.50 ± 0.07	55.5 ± 2.9	2.13 ± 0.32	15.7 ± 1.7	0.63 ± 0.09

WT: perfused with 10 μM glycine, 5 mM PMTS in applicable experiments.
S267C: perfused with 10 μM glycine, bound PMTS in applicable experiments.
Data are the mean values ± SEM from 3-7 patches.

3.2.4 ANALYSIS OF CHANNEL CLOSED DWELL TIMES

Closed dwell time data for each patch were binned based on closed time durations. The resulting histograms for all experimental conditions were fit with five exponential functions (**Figure 3.5**). Channel closed times are important for defining the durations of activations of single ion channels and used to calculate a τ_{crit} to divide the data into bursts of openings. All WT closed-time histograms showed a clear temporal divide between the third and fourth-longest closed channel lifetimes, separating the intraburst from the interburst data. Based on this separation it appears that there are three intra-burst closed times and two longer-lived inter-burst closed times. The longer burst durations varied considerably among patches reflecting heterogeneity in the numbers of channels per patch. In contrast to the WT receptor, the S267C GlyR does not show this clear temporal separation between the third and fourth closed times. However, we believe that the S267C GlyR also has three intra-burst closed times. The first three closed dwell time components show consistency from patch to patch for S267C GlyR in the absence and presence of PMTS similar to WT receptors in the absence and presence of PMTS (**Table 3.2**) suggesting they represent intraburst components. The last two components varied considerably among patches suggesting these represent the longer-lived inter-burst closed times. The addition of PMTS on WT receptors had no effect on closed dwell times [τ_1, $t(6) = 1.11$, $p > 0.3$; τ_2, $t(6) = 1.61$, $p > 0.2$; τ_3, $t(6) = 0.91$, $p > 0.4$; τ_4, $t(6) = 0.44$, $p > 0.7$; τ_5, $t(6) = 0.81$, $p > 0.5$] as shown in **Figure 3.6 A**. The durations of the second and third intra-burst closed τs [τ_2, $F(2, 16) = 10.6$, $p < 0.002$); τ_3, $F(2, 16) = 6.17$, $p < 0.015$] were longer in the S267C mutant than WT GlyR, however, the addition of PMTS had no effects on closed dwell times on S267C receptors. We were only interested in the intra-burst closed times (reflecting activity from a single channel) so we normalized the

likelihood values for the three closed times within bursts (**Figure 3.6 B**). The shortest-lived closing events were more prevalent in the WT receptors [$F(2, 16) = 7.78$, $p < 0.005$], while the longest-lived closing events were more prevalent in both S267C GlyR (with and without PMTS) [$F(2,16) = 19.38$, $p < 0.001$]. PMTS had no additional effects on channel opening likelihoods in the WT [a_1, $t(6) = 0.99$, $p > 0.4$; a_2, $t(6) = 0.99$, $p > 0.4$; a_3, $t(6) = 0.65$, $p > 0.5$] or S267C GlyR.

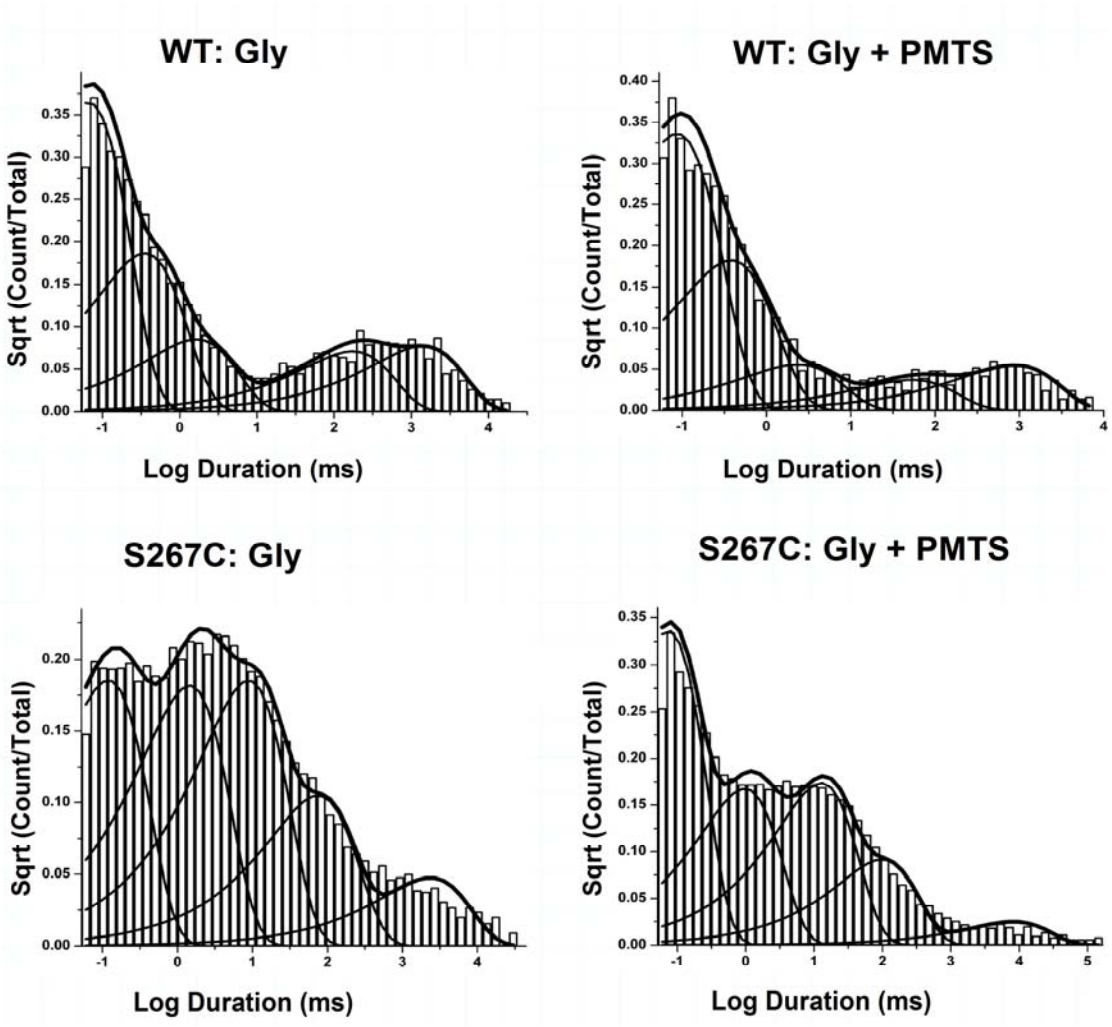

Figure 3.5 Representative closed dwell-time histograms

Each condition was fit using five closed-time components (τs). τ_{crit} values were chosen for each patch based on the fit of the exponential functions to minimize the overlapping area between the tails of intraburst and interburst closing components. For WT GlyR this corresponded to the distinct valley between closed durations three and four. For S267C additional criteria were used to select the τ_{crit} value since no distinct valley occurs. For all conditions τ_1, τ_2, and τ_3 were assumed to represent intra-burst closed durations while τ_4 and τ_5 lie outside of bursts.

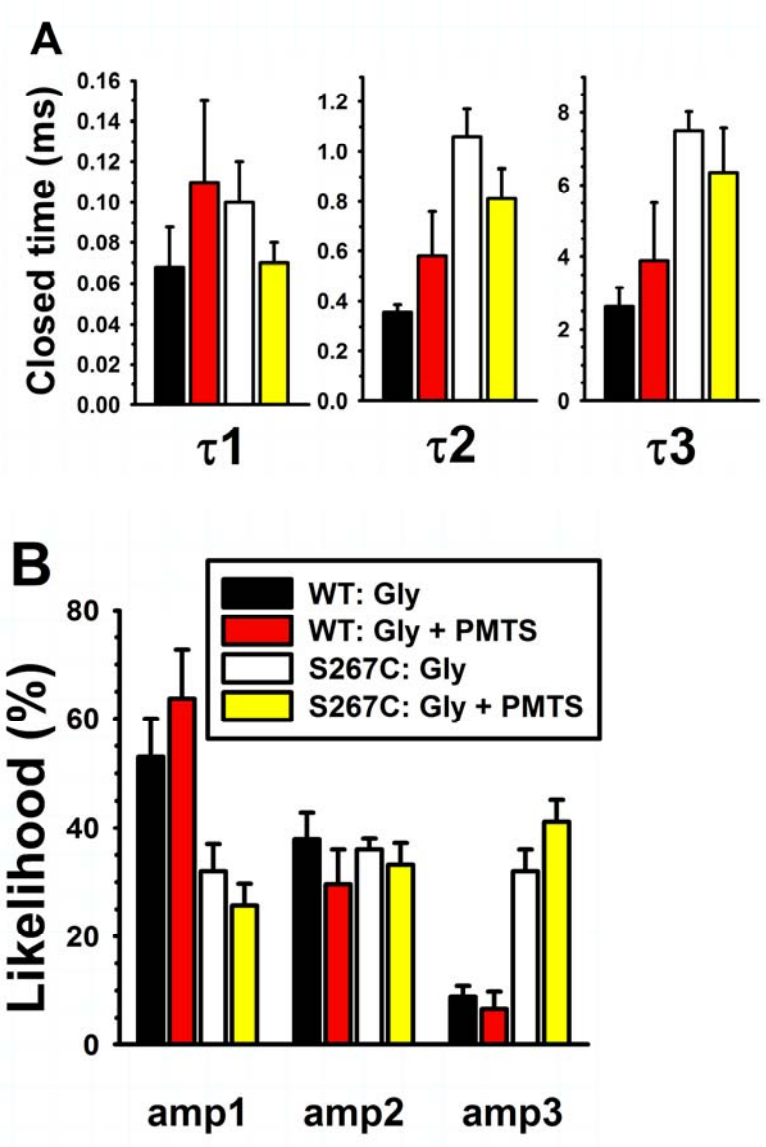

Figure 3.6 Analysis of channel closed dwell times
(A) S267C GlyR displayed longer intra-burst closed dwell times compared to WT for both τ_2 and τ_3 but the addition of PMTS produced no additional effects on the receptor. (B) The likelihood values for the three closed components within bursts were normalized. The shortest-lived closing events were more prevalent in the WT receptors, while the longest-lived closing events were more prevalent in the S267 GlyR. PMTS had no effects on channel closing likelihoods in S267C GlyR. Data represent the mean ± S.E.M. obtained from 3 – 7 patches.

Table 3.2 Closed dwell time analysis

	Tau (ms) and (area %) closed dwell times				
Condition	**τ_1 (ms) (a_1 %)**	**τ_2 (ms) (a_2 %)**	**τ_3 (ms) (a_3 %)**	**τ_4 (ms) (a_4 %)**	**τ_5 (ms) (a_5 %)**
WT	0.07 ± 0.02 (46.2 ± 7.2)	0.36 ± 0.03 (32.2 ± 3.7)	2.62 ± 0.53 (7.5 ± 1.3)	120.51 ± 22.96 (8.3 ± 1.9)	791.43 ± 179.41 (5.8 ± 1.7)
WT PMTS	0.11 ± 0.04 (57.2 ± 10.4)	0.58 ± 0.18 (25.8 ± 5.0)	3.88 ± 1.63 (5.6 ± 2.3)	100.16 ± 47.12 (7.6 ± 4.1)	564.62 ± 202.42 (3.8 ± 1.4)
S267C	0.10± 0.02 (26.1 ± 4.1)	1.06 ± 0.11 (29.6 ± 2.6)	7.5 ± 0.51 (25.5 ± 3.1)	111.35 ± 25.48 (14.0 ± 2.6)	2347.09 ± 914.68 (4.8 ± 1.6)
S267C PMTS	0.07± 0.01 (22.8 ± 3.6)	0.81 ± .12 (29.5 ± 4.3)	6.35 ± 1.24 (35.7 ± 3.2)	43.98 ± 8.41 (11.1 ± 2.6)	2734.96 ± 1008.76 (0.80 ± 0.2)

WT: perfused with 10 μM glycine, 5 mM PMTS in applicable experiments.
S267C: perfused with 10 μM glycine, bound PMTS in applicable experiments.
Data are the mean values ± SEM from 3-7 patches.
Note: in this table the amp (area %) values were normalized among all five (not just the first three) closed times.

3.2.5 S267C EXHIBITS TWO MODES OF ACTIVITY IN THE PRESENCE OF PMTS

The S267C GlyR mutant exhibits two major modes of activity in the presence of PMTS: a high P_o mode (high), which was open 80% of the time during a cluster and a low P_o mode (low), which had a 6% open time. The two distinct modes were often seen within the same cluster, indicating that individual channels could switch between them (**Figure 3.7 A**). The two modes were first separated by chopping the PMTS data into clusters using the τ_{crit} that fell between the fourth- and fifth-longest closed-time τs ($\tau_{crit\text{-}cluster}$) because the longest closed component (τ_5) was thought to represent inter-cluster closed times while the fourth-longest component (τ_4) represents intra-cluster, but inter-burst, closed times. The clusters were then separated based on P_{open} using the K-Means random algorithm within QuB. Once the clusters were separated and analyzed in isolation each mode could be fit by four open and four closed (**Figure 3.7 B**) exponential functions. This made it possible to determine the τ_{crit} that defines burst termination ($\tau_{crit\text{-}burst}$). Operationally we defined bursts of channel opening activity as either single or multiple opening events bounded on both sides by closed periods longer than $\tau_{crit\text{-}burst}$. The markedly different channel opening properties obtained with PMTS on S267C patches necessitated analyzing the two burst modes separately. Both high and low P_o modes were observed in all seven patches studied, but only three of the patches contained sufficient numbers of high P_o opening events for analysis. For each experimental condition we thus calculated for every patch the $\tau_{crit\text{-}burst}$ that fell between the third and fourth closed dwell-time τs and used these values to chop data into bursts. For WT the $\tau_{crit\text{-}burst}$ value was 6.63 ± 0.71 ms and 7.62 ± 1.29 ms in the presence of PMTS. S267C in the absence of PMTS had a $\tau_{crit\text{-}burst}$ of 18.8 ± 2.65 ms. S267C PMTS high mode had a $\tau_{crit\text{-}burst}$ value of 11.1 ± 3.45 ms and 14.25 ± 2.52 ms for low P_o mode.

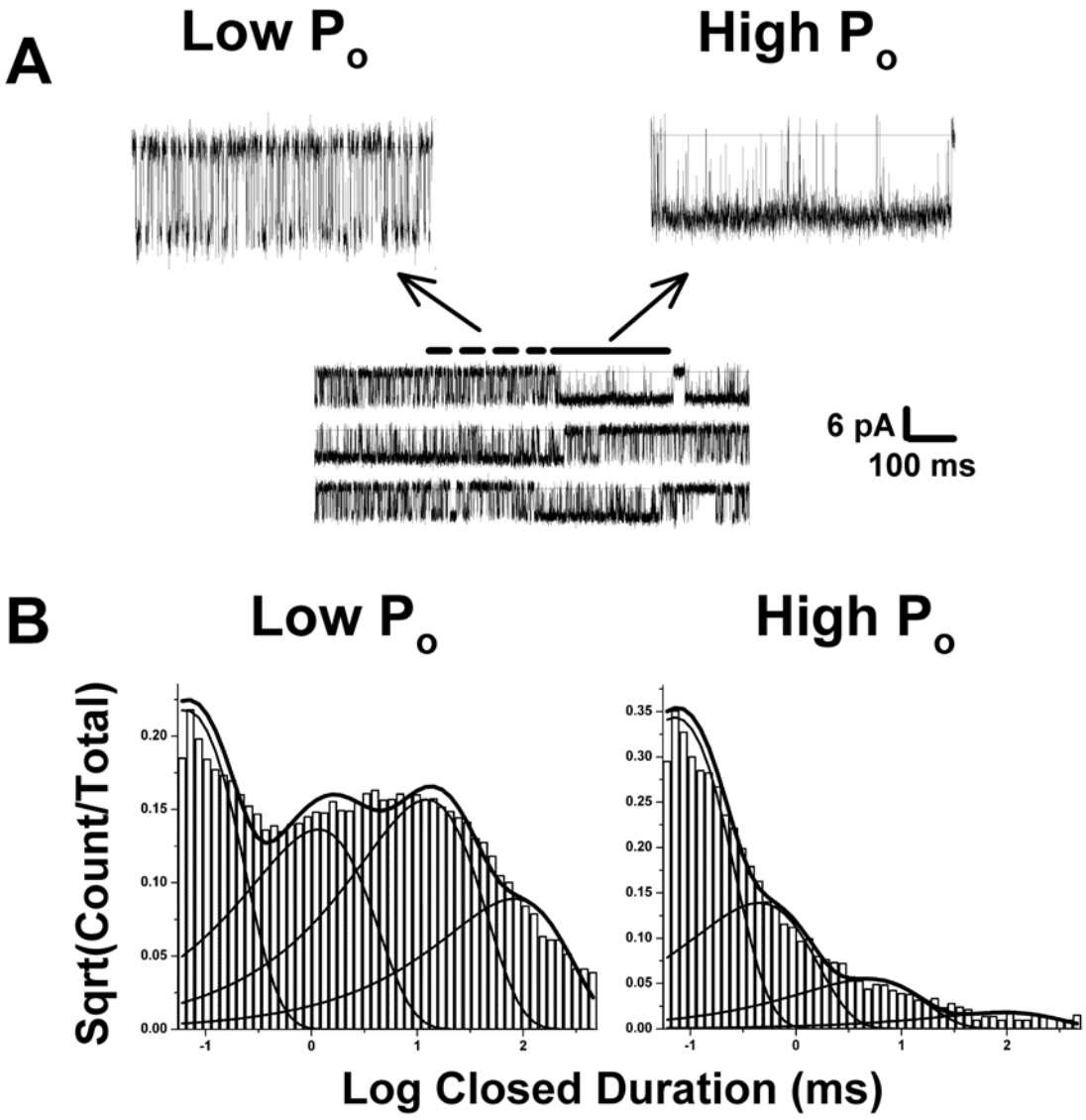

Figure 3.7 S267C exhibits low and high P_o modes in the presence of PMTS
(A) Representative single channel tracings of the two distinct burst modes seen with S267C in the presence of PMTS. The arrow from the dashed line shows a magnified region of low P_o mode while the solid line indicates an example of high P_o mode. (B) Representative closed-time histograms of low P_o (left) and high P_o (right) clusters in the presence of 10 μM glycine plus bound PMTS. Both were best fit with four exponential functions.

3.2.6 BURST DURATION INCREASES IN THE PRESENCE OF PMTS

Patch activity was chopped into bursts using the $\tau_{crit\text{-}burst}$ values determined for each patch in each experimental condition as described above. The burst data were binned according to duration to create histograms (**Figure 3.8**). WT GlyR patches in the absence and presence of PMTS required four exponential functions to provide an adequate fit. The S267C mutant in the absence or presence (high and low P_o) of PMTS required three components to describe the burst data (**Table 3.3**).

WT GlyR showed a modest but non-significant increase [$t(6) = 1.41$, $p > 0.2$] in burst duration in the presence of PMTS (**Figure 3.9**). In the presence of PMTS, the high P_o mode in the S267C mutant increased mean burst duration almost eight-fold [$F(3, 19) = 47.45$, $p < 0.001$] compared to S267C and WT. For the low P_o mode the mean burst duration was not significantly longer in the presence of PMTS compared to the S267C control.

The shortest burst lifetimes (τ_1 in **Figure 3.10 A**) did not vary among the WT, S267C and the two S267C + PMTS modes [$F(3, 19) = 0.88$, $p > 0.47$]. However, with S267C there was a trend towards an enhancing effect of PMTS on τ_2 and a clear increased burst duration produced by PMTS in the high P_o τ_3 group [$F(3, 19) = 32.6$, $p < 0.001$]. Similarly, PMTS increased the longest WT burst duration (τ_4), although not significantly [$t(6) = 1.03$, $p > 0.3$]. No significant differences were seen in the five groups in the likelihoods of observing the three shortest burst components amp_1 - amp_3 (**Figure 3.10 B**).

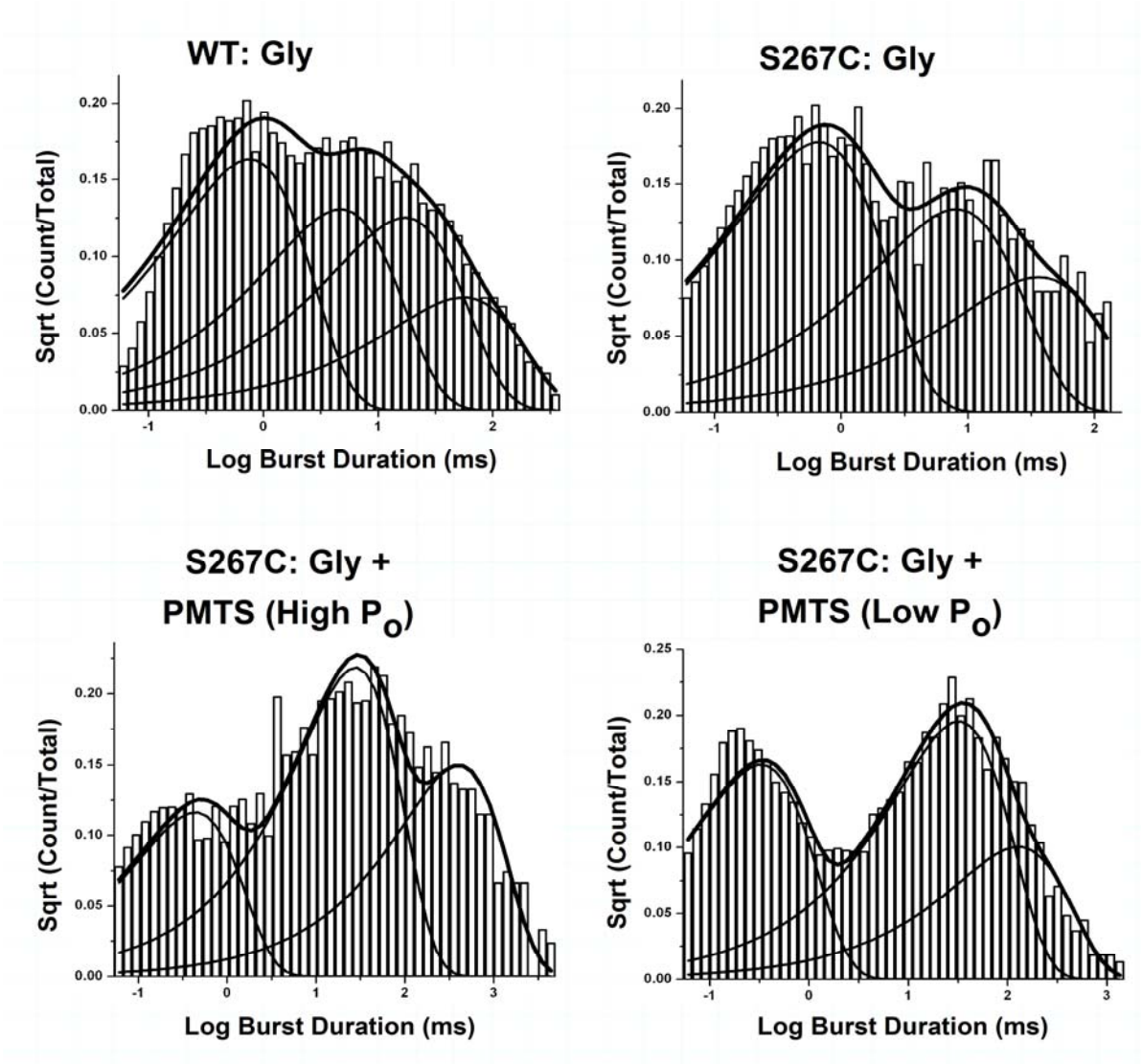

Figure 3.8 Representative burst duration histograms
10 μM glycine applied to WT GlyR in the absence (top left) or presence of PMTS (not shown) required four exponential functions for an adequate fit. S267C GlyR in the presence of 10 μM glycine (top right) was best fit with three exponentials. Both S267C high (bottom left) and low (bottom right) P_o mode in the presence of PMTS were also best fit with three exponentials.

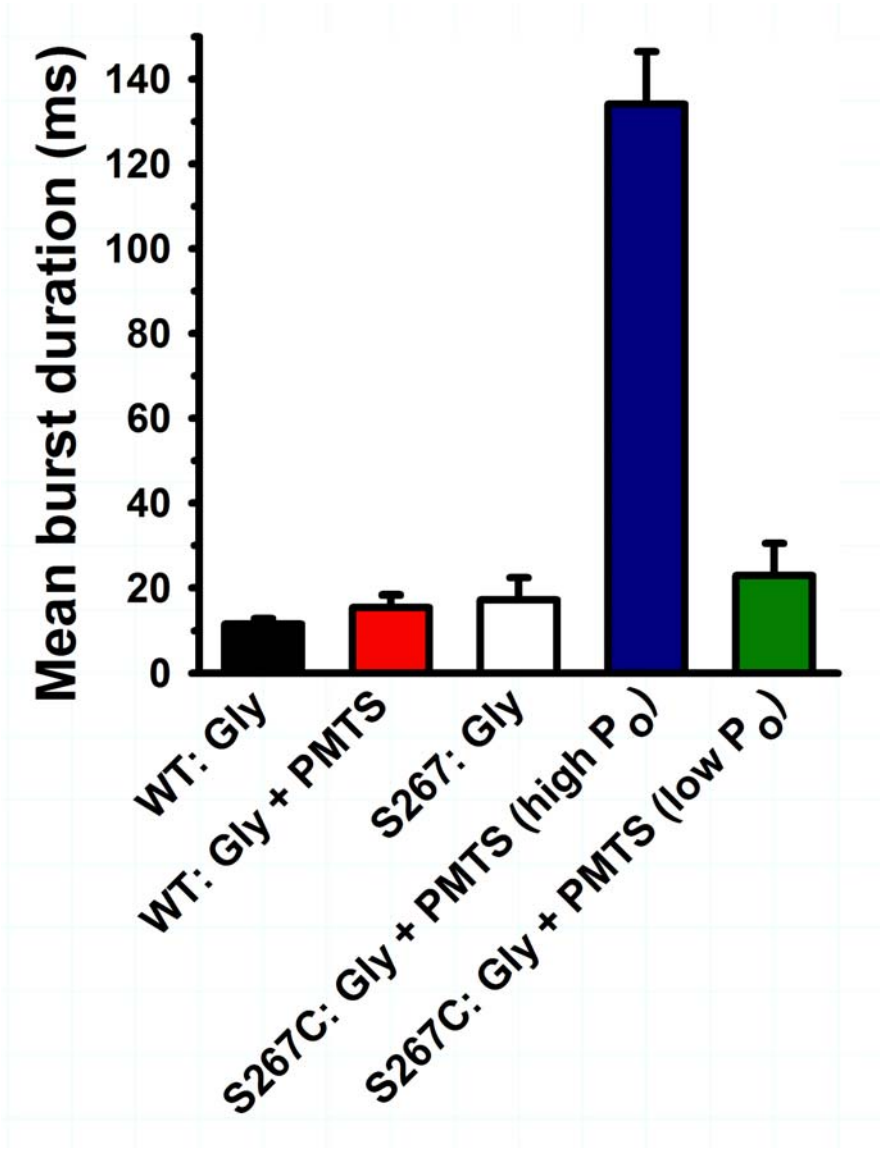

Figure 3.9 PMTS increases mean burst duration
The mean burst duration in the S267C mutant increased from 17.3 ± 5.1 ms in the presence of 10 μM glycine alone to 134.1 ± 12.3 ms in high P_o PMTS mode. PMTS low P_o mode (22.8 ± 7.6 ms) had a similar mean burst duration to S267C glycine alone. WT GlyR (11.6 ± 1.3 ms) increased to 15.5 ± 2.9 ms in the presence of PMTS.

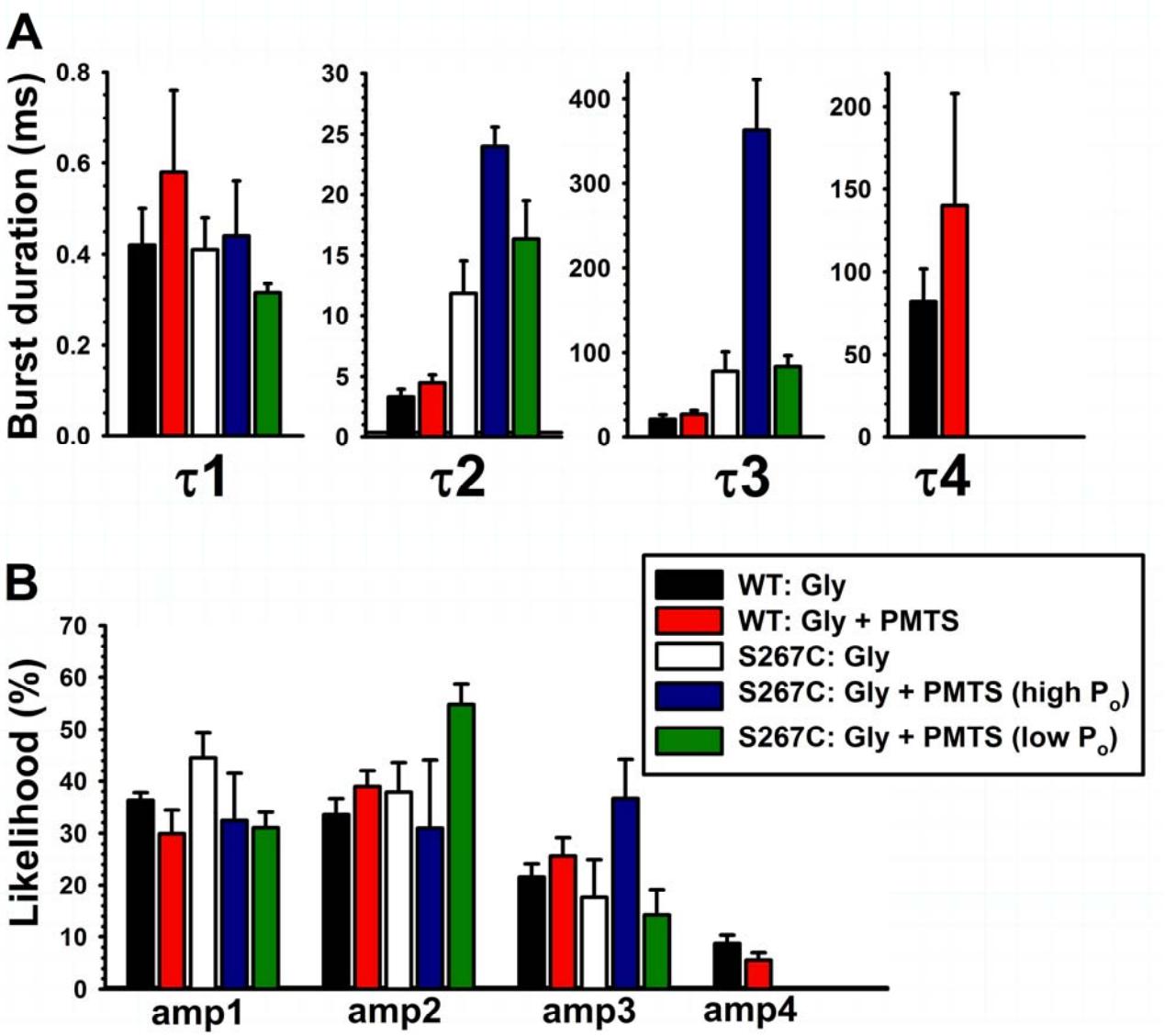

Figure 3.10 Burst duration analysis
(A) PMTS increases burst durations by increasing burst time constants. PMTS increases the durations of the longer-lived burst components; specifically the longer-lived τ_3 component for S267C and τ_4 for WT GlyR. (B) The likelihood of entering a particular burst component was not changed among the experimental conditions.

Table 3.3 Burst duration analysis

	Tau (ms) and (area %) Burst Durations				
Condition	**τ_1 (ms) (a_1 %)**	**τ_2 (ms) (a_2 %)**	**τ_3 (ms) (a_3 %)**	**τ_4 (ms) (a_4 %)**	**Mean Burst Duration (ms)**
WT	0.42 ± 0.08 (36.3 ± 1.5)	3.32 ± 0.65 (33.5 ± 3.1)	20.7 ± 5.4 (21.6 ± 2.5)	81.85 ± 20.01 (8.7 ± 1.6)	11.56 ± 1.34
WT PMTS	0.58 ± 0.18 (29.9 ± 4.5)	4.48 ± 0.67 (39.0 ± 3.1)	26.5 ± 4.6 (25.6 ± 3.5)	139.82 ± 68.03 (5.6 ± 1.4)	15.47 ± 2.91
S267C	0.41 ± 0.07 (44.5 ± 4.8)	11.85 ± 2.70 (37.9 ± 5.8)	77.8 ± 23.2 (17.6 ± 7.3)	N/A	17.29 ± 5.10
S267C PMTS high P_o mode	0.44 ± 0.12 (32.4 ± 9.1)	23.99 ± 1.59 (30.9 ± 13.1)	363.3 ± 59.1 (36.6 ± 7.6)	N/A	134.09 ± 12.31
S267C PMTS low P_o mode	0.31 ± 0.02 (31.0 ± 3.0)	16.38 ± 3.10 (54.7 ± 4.0)	83.5 ± 13.2 (14.2 ± 4.9)	N/A	22.83 ± 7.63

WT: perfused with 10 μM glycine, 5 mM PMTS in applicable experiments.
S267C: perfused with 10 μM glycine, bound PMTS in applicable experiments.
Data are the mean values ± SEM from 3-7 patches.

3.2.7 PMTS AFFECTS BURST PROPERTIES

The primary effect of the S267C mutation on burst properties was to increase the percentage of longer-lived bursts compared to the WT α1 GlyR (**Figure 3.11 A** left panel). In addition, in the high P_o mode, PMTS application resulted in bursts considerably longer and more prevalent than those produced by glycine alone in the S267C mutant (**Figure 3.11 A** right panel). For example, while bursts longer than 50 ms represent 6% of the total bursts seen when glycine is applied alone to WT receptors (7% in the presence of PMTS, not shown) this increases to 9% when applied to the S267C GlyR. After the addition of PMTS, they comprise 16% of all S267C bursts (not shown), which is composed of 35% in the high P_o condition and 10% in the low P_o mode.

PMTS appeared to decrease the likelihood of observing isolated single opening events in S267C GlyR, although this effect was not statistically significant [$F(3,19) = 2.56$, $p>0.09$] compared to S267C alone or WT GlyR. In the WT receptor 32% of bursts consisted of single openings, which dropped to 21% in the presence of PMTS [$t(6) = 2.35$, $p > 0.06$]. In the S267C mutant this value was 34% and decreased to 18% in the high P_o PMTS group and to 24% in the low P_o PMTS group (**Figure 3.11 B**).

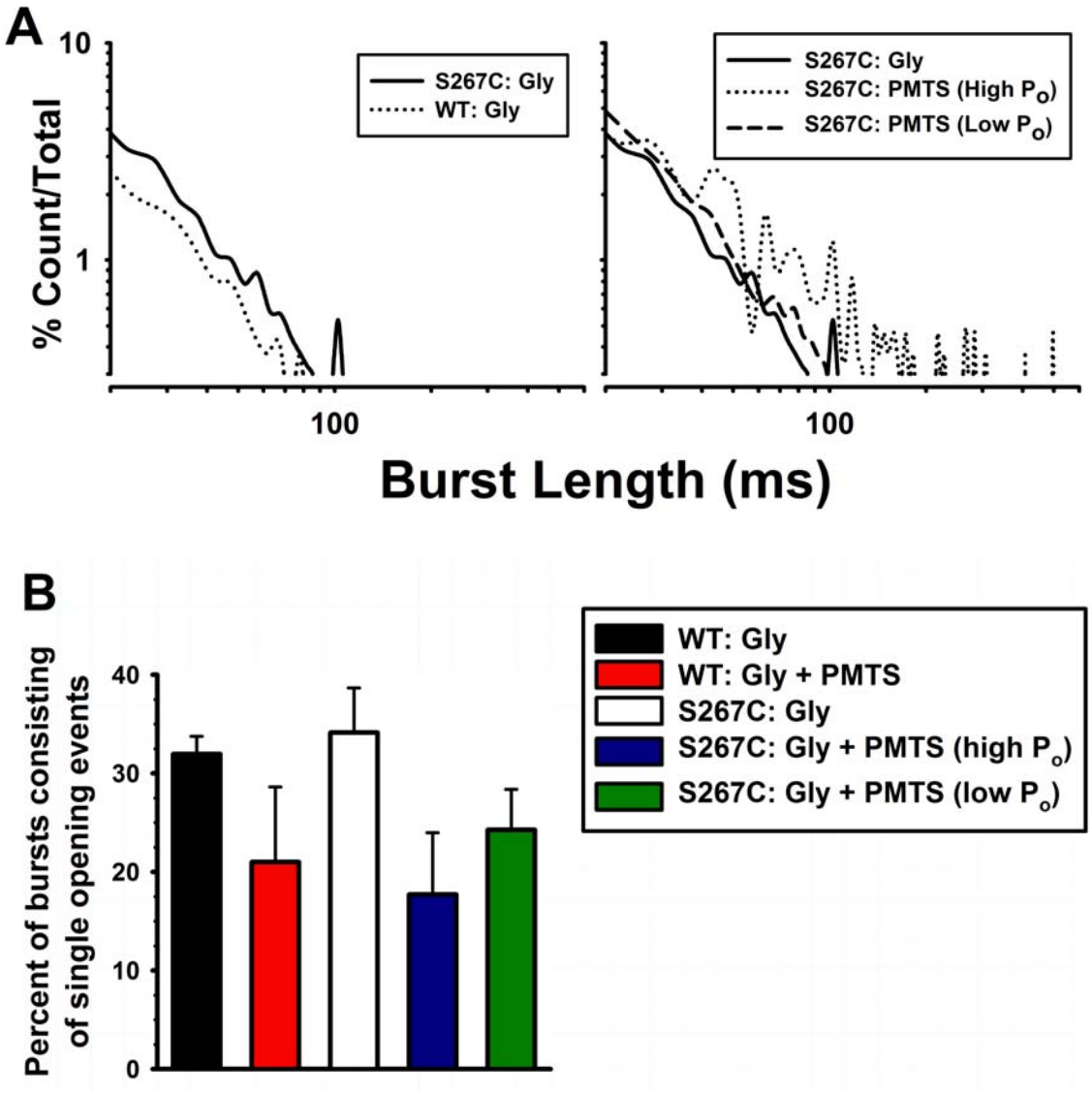

Figure 3.11 PMTS affects burst properties
(A) PMTS increases the duration of bursts. Burst lengths were combined from all patches for each experimental condition; the abscissa represents burst length while the ordinate represents the percentage of bursts counted. The S267C mutant increased the percentage of longer-lived bursts compared to WT (left panel) while PMTS (high P_o mode) resulted in bursts considerably longer and more prevalent (right panel). (B) There was a trend toward a decrease in the likelihood of single opening events in the presence of PMTS for both WT and S267C GlyR. Data represent the mean ± S.E.M. obtained from 3 – 7 patches.

3.2.8 INTRABURST PROPERTIES

The number of opening events per burst was obtained for each patch by dividing the number of opening events by the number of bursts. Data from all the patches for each condition were averaged together to get the mean numbers of openings per burst (**Figure 3.12 A**). WT GlyR showed an increase, although not significant [$t(6) = 1.17$, $p > 0.3$], in openings per burst from 15.9 ± 5.0 to 33.0 ± 17.7 in the presence of PMTS. S267C GlyR averaged 8.6 ± 2.5 openings per burst. This increased to 129.8 ± 39.0 in the high P_o PMTS group while the average number of openings per burst in the low P_o PMTS group was 12.0 ± 2.4. The high P_o PMTS group showed a significantly greater numbers of openings per burst than the other S267C groups and WT [$F(3,19) = 18.88$, $p < 0.001$].

The weighted P_{open} within bursts was also determined (**Figure 3.12 B**) by dividing the total open time by the sum of burst lengths. There was no change with WT in the absence or presence of PMTS [$t(6) = 1.14$, $p > 0.3$]. However, the S267C mutation decreased the intraburst P_{open} compared to WT [$F(3, 19) = 54.16$, $p < 0.001$]. When the P_{open} within bursts was calculated for the entire PMTS data set there was no change compared to S267C (not shown). When the modes, which were separated based on P_o, were examined individually the PMTS high P_o mode showed a significant increase compared to S267C glycine alone, while the low P_o mode showed no change.

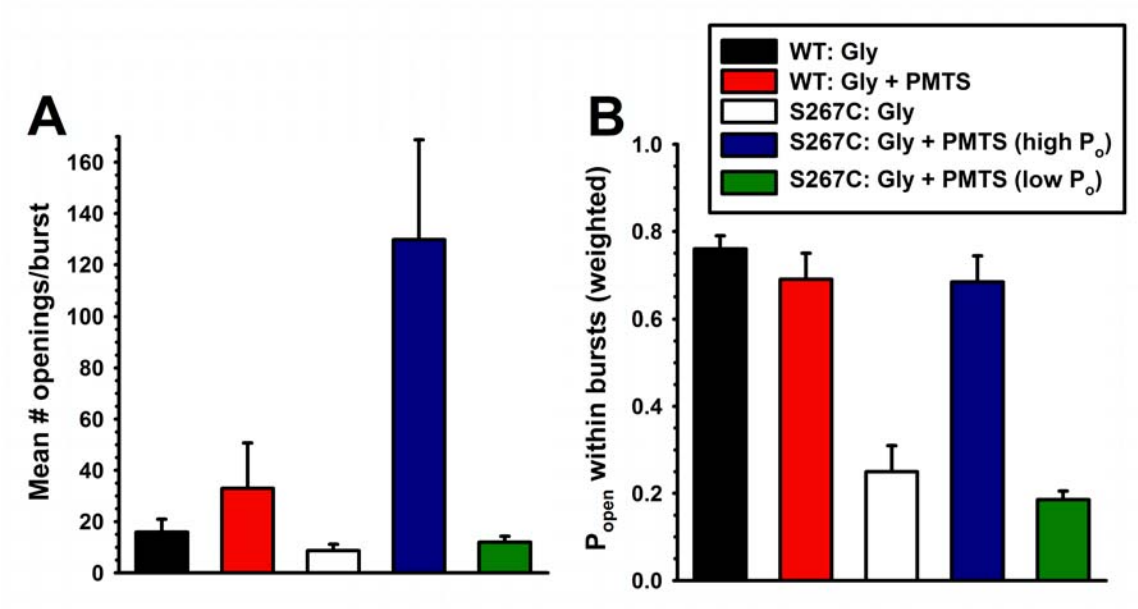

Figure 3.12 PMTS affects intraburst properties
(A) The mean number of opening events in each burst was calculated and averaged to obtain the unweighted mean number of openings per burst. In WT and high P_o mode S267C PMTS increased the number of openings that occur during a burst. (B) The S267C mutation decreases the weighted intraburst P_{open} compared to WT. PMTS applied on WT and S267C low P_o mode produced no changes in P_{open}. However, PMTS high P_o mode increased the P_{open} within bursts compared to the S267C mutant.

3.3 Discussion

3.3.1 WT GLYR DATA IN THE ABSENCE AND PRESENCE OF PMTS

Before investigating our hypothesis that PMTS labeling of the S267C residue mimics the effects of alcohol binding on GlyR function we first needed to make single channel recordings of WT GlyR and observe the effects of PMTS on WT cells. Our WT results with 10 μM glycine were compared to those of the Colquhoun and Sivilotti labs at University College London. Their extensive investigations (Colquhoun and Sivilotti, 2004; Lape et al., 2008) using single channel recordings from α1 homomeric GlyR at multiple glycine concentrations have provided the necessary foundation for our work. Experiments utilizing multiple agonist concentrations are most comprehensive but our analysis was limited to a low concentration of glycine since enhancement by allosteric modulators only occurs in the presence of low concentrations of glycine. Our ultimate goal was to compare our S267C GlyR mutant PMTS data to the ethanol results obtained by Welsh et al. (2009) and look for similarities in the single channel parameters measured. There is no effect of ethanol at maximal glycine concentrations (Mascia et al., 1996) but it is possible that PMTS affects the maximal current for S267C GlyR, as measured in whole-cell experiments, due to the fact that it increases conductance (Michelle Dupre, personal communication). As a result, only low glycine concentrations were used in this study.

Previous single channel studies have reported that the GlyR has up to six conductance states (Hamill et al., 1983). Beato et al. (2002) found the GlyR had two conductance states (35-45 pS and 60-90 pS) that did not depend on agonist concentration. We also saw two conductance states for WT GlyR, which consisted of a predominant main conductance, and an infrequent (< 10%) subconductance. Both of these

conductance values were also observed in the presence of PMTS. Following the precedence set by Beato et al. in the 2002 paper we idealized our data without a distinction between the subconductance levels. The mutation to S267C produced a shift in preference of channel opening to the "subconductance state" we saw in WT GlyR. The subconductance state predominated in the mutant, although openings to the full conductance level were also occasionally observed during recordings. This likely explains the lower currents observed after application of maximally effective concentrations of glycine to S267C GlyR, compared to those seen in WT receptors (Roberts et al., 2006). Interestingly, the covalent binding of PMTS seemed to reverse this and openings returned predominantly to the same main conductance as WT, although there were also infrequent openings to a subconductance level (**Figures 3.1 & 3.2**). When the PMTS data were separated into high and low P_o modes there was no difference in the conductance observed between the two modes, with both opening to a main conductance of ~100 pS.

Beato and colleagues (2002) performed outside-out single channel electrophysiology on HEK 293 cells and fit their patch data with four open components in the presence of 10 μM glycine. The time constants and relative areas were: τ_1, 0.054 ms (8 %); τ_2, 0.48 ms (30 %); τ_3, 1.4 ms (46 %); τ_4, 4.7 ms (17%). Our data was best fit with only three open components likely due to limitations of the recording equipment not being able to resolve the fastest time constant and our imposed dead time of 60 μs. Our first time constant therefore probably represents a combination of τ_1 and τ_2 reported by Beato et al. (2002). Our time constants and relative areas were similar to their findings at: τ_1, 0.27 ms (44 %); τ_2, 1.3 ms (45%); τ_3, 5.2 ms (11%). The mean open time stated by Beato et al. (2002) was 1.7 ms compared to our reported 1.2 ms (**Figures 3.3; 3.4 A-C**). Beato et al. (2002) observed that the mean open time increased as the glycine

concentration increased from 0.3 μM to 10 μM. This was due to an increase in relative area of the longer-lived components and a decrease in shorter-lived components, not a change in time constants, which remained stable across all concentrations tested. At higher glycine concentrations longer openings occurred more frequently but had the same durations. In the presence of PMTS the time constants, amplitudes, and mean open time stayed consistent compared to WT patches in the presence of only glycine. This lack of effect suggests that, unlike increasing concentrations of glycine, PMTS does not stabilize the GlyR open states.

Like Beato et al. (2002), we also observed three shut times within bursts. Their time constants and relative areas were: τ_1, 0.037 ms (37 %); τ_2, 0.38 ms (48 %); τ_3, 2.6 ms (14 %) comparable to our data with the following values: τ_1, 0.067 ms (53 %); τ_2, 0.36 ms (38 %); τ_3, 2.6 ms (9 %). They found that their time constants and areas were not affected by agonist concentration. We also found that in the presence of PMTS our closed dwell time values remained consistent compared to glycine alone on WT (**Figures 3.5; 3.6 A & B**).

A $\tau_{crit\text{-}burst}$ value for both Beato et al. (2002) and our data was calculated between the third and fourth closed-time components, showing consistency with our findings. The average $\tau_{crit\text{-}burst}$ value Beato et al. (2002) used for chopping data into bursts at 10 μM glycine was 5.8 ms verses our 6.6 ms. Beato et al. (2002) fit their burst length distributions at 10 μM glycine with five exponentials while we only used four components for the best fit. Their burst length values were: τ_1, 0.068 ms (17 %); τ_2, 0.62 ms (33 %); τ_3, 3.8 ms (31 %); τ_4, 15.7 ms (18 %); τ_5, 69.3 ms (4 %) compared to our data with the following values: τ_1, 0.42 ms (36 %); τ_2, 3.3 ms (33 %); τ_3, 20.7 ms (22 %); τ_4, 81.9 ms (9 %). Again, it appears we were unable to observe the fastest tau component, which explains why we needed fewer components to fit the data. Our fourth burst

component is longer and occurs more frequently and is partially accountable for our mean burst duration of 11.6 ms being higher then Beato et al. (2002) 7.1 ms mean (**Figures 3.8; 3.9; 3.10 A & B)**. In the presence of PMTS our mean burst duration increased slightly due to an even longer τ_4 component. This is in contrast to Beato et al. (2002) who found that the tau lifetimes remained consistent across glycine concentrations while the areas changed.

The mean number of openings per burst for Beato et al. (2002) data at 10 μM glycine was 3.5, which differs from our 15.9. However, the Beato et al. (2002) paper utilized three geometric components to fit the distribution of the number of openings per burst and to calculate the mean. This is in contrast to our arithmetic method, which might account for the difference. Beato et al. (2002) found that the mean number of openings per burst increased as the glycine concentration increased; the lifetimes of each component did not change while the areas did. We observed an increase in the number of open events per burst in the presence of PMTS. This suggests that, because bursts last for a longer duration in the presence of PMTS, there is more time available for openings to occur (**Figure 3.12 A**). Beato et al. (2002) also found a decrease in the number of bursts composed of single opening events as the concentration of glycine increased. This is similar to our findings in the presence of PMTS where there are more bursts containing multiple openings (**Figure 3.11 B**).

We found our data to be consistent with Beato et al. (2002) and were able to use our WT GlyR data as a baseline and compare it to our findings of glycine co-applied with PMTS on WT receptors. Previous findings at the whole cell level showed potentiation of WT GlyR responses in the presence of PMTS (Mascia et al., 2000). Experiments by Roberts et al. (2006) showed that 5 mM PMTS caused significant enhancement of WT GlyR current when co-applied with EC_{10} glycine. Despite this, using *t*-tests to compare

our data in the absence or presence of PMTS on WT GlyR we were unable to tease out an effect for any of the single channel parameters tested. This could be due to the low number of patches tested or our concentration of PMTS, based on whole cell studies, not being appropriate. The experiments were conducted in the steady state, so PMTS was applied continuously over the WT GlyR cells. This might have had a detrimental effect on the viability of the cell being tested which could lead to shortened recording times and low event activity. Despite this, we did see trends that led us to believe that under the right conditions there would be increased enhancement of WT GlyR current seen at the single channel level, similar to the results using whole-cell electrophysiology. There was a slight increase in mean burst duration due to an increase in the burst time constants, especially the longest-lived component. There was also a decrease in the number of bursts consisting of single opening events and an increase in the mean number of openings per burst. These are the same major changes that occur in the presence of ethanol on WT GlyR (Welsh et al., 2009) and although our results were not significant, the trends observed in the data are encouraging.

However, the main focus of the work was to use an alcohol analog with permanent binding at a defined molecular location, so despite the drawback of not having a significant PMTS effect on WT GlyR, this did not affect the overall outcome of the project. We were able to see differences with the S267C mutation in the absence and presence of PMTS and utilized 1-way ANOVAs to compare the three (WT, S267C, S267C PMTS) experimental conditions.

3.3.2 WT DATA COMPARED TO S267C IN THE ABSENCE AND PRESENCE OF PMTS

Although S267C open dwell time histograms in the absence and presence of PMTS were also best fit by the sum of three exponential functions, the mutation to

S267C caused a few minor alterations in receptor function compared to WT. In addition to the changes we saw in conductance (**Figure 3.2**), there was a significant decrease in the S267C mean open time compared to WT that was not further changed by PMTS. This change can be attributed to a decrease in the two shortest time constants, caused by the mutation. PMTS did increase the likelihood of opening to the longest time component for S267C compared to S267C alone or WT (**Figure 3.4 A-C**).

Similar to WT, the S267C GlyR had three intraburst closed components but the closed time tau values were longer and occurred more often (**Figure 3.6 A & B**). The addition of PMTS produced no additional effects on channel closed dwell times and likelihoods and the data were relatively consistent when compared with S267C. The lack of effect supports the idea that PMTS does not modulate the GlyR by stabilizing the open states.

The S267C GlyR mutant displayed two modes of activity in the presence of PMTS that were not observed in any of the other experimental conditions (**Figure 3.7 A**). Receptors exhibiting different modes of activity have been observed before. Lema and Auerbach (2006) expressed α1β1γ2S GABAR in HEK 293 cells and found, at all GABA concentrations tested, three different gating patterns discernible by open probability. Additionally, Keramidas and Harrison (2008) saw up to three different bursting modes distinguishable by open probability in α1β2γ2S $GABA_AR$ when activated by saturating concentrations of GABA. Like these other labs we also separated our data based on P_o (high and low modes) and were able to show an effect of PMTS that was greater then when the PMTS data were viewed as one group. Breaking the data into clusters also helped determine what components were intra-burst, intra-cluster but inter-burst, or inter-cluster. There were more closings of short duration in the high P_o mode compared to low P_o mode, which had a smear of closed duration events with longer closings more

prevalent (compared to high P_o mode). This explains why there was no clear temporal separation seen with S267C PMTS closed-dwell time histograms (**Figures 3.5; 3.7 B**).

The major effect of the S267C GlyR high P_o PMTS mode was a significant increase in mean burst duration (**Figure 3.9**). This was clearly seen visually during recordings as channel activity occurred for much longer periods of time compared to the other experimental conditions (**Figure 3.1**). This increase is attributed to increasing burst time constants, specifically the longer-lived burst components, while the likelihoods remained unchanged (**Figure 3.10 A & B**). When PMTS is bound in high P_o mode burst lengths are considerably longer and more prevalent (**Figure 3.11 A**) compared to S267C or WT in the presence of glycine alone. Accordingly, high P_o PMTS mode also had the fewest bursts that consisted of single openings (**Figure 3.11 B**). Although a burst of long duration is just as likely to occur for any of the experimental conditions, when it does occur with high P_o PMTS mode it lasts for a longer duration. Additionally, since the bursts occur for a longer period of time in S267C high P_o PMTS mode there is a greater opportunity for multiple openings to occur (**Figure 3.12 A**).

A major difference between WT and S267C GlyR was the change in P_{open} (**Figure 3.12 B**). The mutation caused a significant decrease in P_{open}, which might be attributed to the decrease seen in mean open time with S267C. The addition of PMTS in high P_o mode seems to restore the P_o. This is a logical conclusion since high P_o mode was selected for based on P_o. Also, when the PMTS data are broken down into modes, the high P_o mode has an increased mean open time compared to the low P_o mode (not shown).

The first step of this project was to conduct outside-out recordings of WT GlyR to make baseline measurements on a variety of single channel parameters described above. The following set of experiments investigated the effects of PMTS on WT receptors. This set the foundation for subsequent projects and allowed us to make valid comparisons. We

next used a GlyR mutant, S267C, and carefully compared its changes in function to WT so that when PMTS was added we could identify what effects were due to the mutation and which were the results of the thiol reagent. Since amino acids critical for alcohol and anesthetic effects were first identified for the GlyR (Mihic et al., 1997), the definitive location of the binding site has been in question. The overall main goal of this project was to add further evidence demonstrating that transmembrane amino acid residue S267 actually constitutes part of an alcohol binding site.

3.3.3 PMTS BINDING AT S267C VERSES ETHANOL BINDING WT GLYR

In this dissertation I present my findings on the effects of PMTS, studied at the single channel level. PMTS was selected since it mimics a small alcohol in size but can permanently bind to an introduced cysteine residue in the S267C GlyR mutant. This enabled us to test the hypothesis that the enhancing effects of ethanol and volatile anesthetics are due to the addition of volume within the TM2-TM3 binding pocket. We would predict that if ethanol acts at this site then the consequences of thiol binding at S267C should mimic ethanol effects on WT GlyR.

We compared several single channel parameters (**Table 3.4**) and found many parallels between PMTS on S267C GlyR and ethanol on WT GlyR. The mean open time of S267C GlyR was not affected by PMTS consistent with the lack of alcohol effects on channel mean open times in WT GlyR (Welsh et al., 2009). Although the mutation to S267C affected some dwell time components, covalent binding of PMTS did not markedly affect either open or closed dwell times, analogous to what was generally also seen with ethanol (Welsh et al., 2009). An anesthetic, but not sub-anesthetic, concentration of ethanol produced an increase in the lifetime of the longest-lived closed component that was not seen with PMTS. The effects produced by PMTS on S267C

GlyR thus cannot be explained by changes in open or closed times, similar to what was previously found for ethanol. Further, the lack of effect of PMTS on channel open lifetimes suggests that, like ethanol, it does not stabilize GlyR open states.

Both PMTS and ethanol produced changes in receptor bursting properties. The high P_o PMTS mode exhibited a mean burst duration significantly greater than the S267C GlyR exposed to glycine alone, due to the significant increase in the longest-lived burst time constant. This is quite similar to the effects of ethanol on WT GlyR, in which ethanol does not affect the duration of the shortest-lived burst component but does increase medium- and longest-lived burst time constants (Welsh et al., 2009). Since the likelihood to enter any of the burst components in the S267C GlyR did not change in the absence or presence of PMTS, the increases in τs must fully account for the increased burst duration produced by PMTS. This too parallels the effects ethanol has on WT α1 GlyR.

PMTS application decreases the percentage of bursts consisting of single opening events; i.e., addition of PMTS favors groupings of openings rather then isolated opening events. This was also seen with ethanol when it was applied to the WT GlyR (Welsh et al., 2009). In addition, PMTS increases the mean number of openings per burst in the high P_o mode, again consistent with the actions of ethanol on WT receptors (Welsh et al., 2009).

Not all of the effects of ethanol observed on WT α1 GlyR were reproduced by PMTS binding at the S267C site. While ethanol does not affect WT GlyR conductance (Welsh et al., 2009), PMTS covalently binding to the S267C GlyR did increase its conductance. Although it restored the conductance to a level similar to WT GlyR this was an unexplained modification. However, it is not surprising that mutating a residue in TM2 so close to the pore might change conductance. Perhaps the covalent addition of

PMTS to the S267C residue makes it behave like a different mutation (eg S267F?) might with respect to conductance. Also, the S267C mutation has an effect on intraburst P_o, which is reversed by the presence of PMTS in the high P_o mode. No change in P_o was seen with ethanol on WT GlyR. However, if the high and low P_o modes are examined as a single PMTS group then the weighted P_o is the same as the S267C GlyR in the absence of PMTS.

Many of the single channel parameters studied showed similarities in the actions of ethanol and PMTS, and those that were different did not affect the overall conclusions. Both ethanol and PMTS applications resulted in increased burst durations. The only parameter measured that consistently changed for both was an increase in the longest-lived burst time constants. This implies that when bursts occur they last for a longer duration.

Although the neutral PMTS reagent has structural similarities to alcohol, there were several differences between the PMTS and ethanol (Welsh et al., 2009) experiments. The ethanol study was done in *Xenopus* oocytes using 3 μM glycine, compared to HEK 293 cells at a concentration of 10 μM glycine for the PMTS experiments. Substituting a cysteine residue for a serine increased the volume of the binding pocket by 13 $Å^3$ (Lobo et al., 2004a). Also, amino acids other than S267 have been identified as playing roles in the alcohol/anesthetic binding pocket (**Section 1.5**). While PMTS was permanently bound to the cysteine residue at position 267, ethanol was free to interact with other residues. With five potential binding sites on an α_1 homologous receptor, PMTS may have been bound at all five sites while ethanol may have only occupied two or three binding sites at a time. Also, PMTS forms a disulfide bond by coupling two thiol groups together and is covalently bound to the cysteine residue while ethanol contains a hydroxyl group that forms hydrogen bonds which can form and break

allowing ethanol to come on and off the binding sites, resulting in a difference in occupancy lifetimes. This may explain why different modes are seen with PMTS but not ethanol application on WT GlyR. We recognize that some of the dissimilarity seen between ethanol and PMTS effects may be attributed to these differences. However, based on the overall consistencies in our results we have provided substantial evidence to further support the hypothesis that ethanol and PMTS seem to share a common binding location at serine-267 in TM2 of the α_1 GlyR.

Table 3.4 Summary table of alcohol effects on WT receptors compared to PMTS effects on S267C GlyR

	Single Channel Parameters	Ethanol WT GlyR	PMTS | (high P_o mode) S267C GlyR
	Conductance	∅	↑
Dwell time Analysis	Mean open time	∅	∅
	Open tau & amps	∅	∅
	Closed tau & amps	∅	∅
Burst Analysis	Tau	↑	↑
	Likelihood	∅	∅
Intraburst Analysis	Bursts with single opening	↓	↓
	Mean # openings/burst	↑	↑
	P_{open}	∅	↑

Ethanol experiment: 200 mM ethanol compared to 3 μM glycine WT control.
PMTS experiment: bound PMTS compared to 10 μM glycine S267C control.

KEY:
∅ No effect compared to glycine control
↑ Increase compared to glycine control
↓ Decrease compared to glycine control

3.3.4 MECHANISTIC MODEL OF THE GLYCINE RECEPTOR

The experiments presented here using PMTS to investigate the alcohol binding site provided a descriptive depiction of GlyR function. However, a mechanistic model is useful for understanding the behavior of an ion channel. A kinetic scheme can describe the probability of each state being occupied and the time course for the model.

Beato and colleagues in 2002 provided a simple activation mechanism for the homomeric α1 GlyR by fitting recordings made at 0.3, 1, and 10 μM glycine concentrations. They devised a well-fit reasonable model consisting of six closed states, linearly connected, and five open states, with each open state connected to only one closed state. This scheme fit the data and logically made sense because each α subunit of the GlyR pentamer possesses a potential binding site. In 2004, they refined the scheme by simultaneously fitting recordings made at various glycine concentrations (10- 1000 μM). They tested different models to find the one that gave the best description of their single channel results. They found that a model with four closed and three open states provided just as good a fit as the previously-tested model. These three open states correspond to the receptor being singly, doubly, or triply liganded with glycine. Maximum gating efficacy was reached despite the receptor possessing two potentially empty binding sites. The best fit was unconstrained, allowing an interaction between binding sites when the receptor was in the closed conformation. The rate constants fitted with this mechanism predicted the observed experimental distributions adequately.

Welsh et al. (2009) found that ethanol enhances burst durations by lengthening the longer burst time constants. The WT and ethanol experiments with 3 μM glycine were fit to a kinetic scheme with three closed and two open states. The k_{-1} rate constant, which describes the rate of burst termination, changed significantly in the presence of

ethanol while all other rate constants remained consistent. This observed rate change in the presence of ethanol begins to describe the actions of ethanol on GlyR function. Due to the similarity of ethanol and PMTS both enhancing burst time constants it is quite possible that PMTS exposure also affects the k_{-1} rate constant. However, detailed modeling experiments comparing WT to S267C in the absence and presence of PMTS need to be undertaken to make any decisive conclusions.

CHAPTER 4 | CONCLUSIONS

4.1 Overview

Ethanol, the type of alcohol found in alcoholic beverages, has a simple molecular formula (C_2H_5OH). Despite its basic structure and widespread use, the mechanism of action of alcohol remains elusive. A large number of putative molecular targets have been suggested to mediate the behavioral effects of ethanol including many enzymes, ion channels, and receptors. Based on current research, we chose to investigate the interaction alcohol has with the GlyR to help understand the molecular cause of alcoholism. Our search for the alcohol binding site on the GlyR, through the use of an alcohol analog, in combination with single channel electrophysiology, advances the field of alcohol research by providing further evidence of a defined binding site for alcohol on this receptor. Continued progress will eventually lead to improved treatments for alcoholism.

We mutated amino acid S267, which is part of the putative alcohol binding pocket (Mihic et al., 1997; Mascia et al., 2000), to facilitate a covalent interaction between a cysteine residue at that site with an alcohol analog. We showed that PMTS is permanently bound at S267C in the mutated GlyR since it dramatically affected GlyR function. Consistent with this residue lining a water-filled cavity, only in this environment can PMTS covalently bind, resulting in irreversible effects on the S267C GlyR. A reversible effect of PMTS on WT GlyR implies that PMTS is only binding to the cysteine introduced at position 267.

The results presented in this dissertation provide insight into the mechanism of alcohol binding on the GlyR. This study was novel because it combined an alcohol analog with single channel electrophysiology using a GlyR mutant. In the absence of structural data for the GlyR, this method gives insight as to where ethanol might bind to the receptor. PMTS covalently binding to a cysteine residue is a valuable tool because any changes observed in GlyR function are due to PMTS interacting with the receptor at that known and specified location. Previously we knew that, like ethanol, PMTS affected GlyR function and now we know that its binding at residue 267 produces enhancement of GlyR function by a mechanism similar to, but not identical with, ethanol.

A cysteine residue is structurally similar to a serine, although the mutation alone did cause changes in GlyR function. However, we were able to control for this by comparing WT GlyR to S267C GlyR in the absence and presence of PMTS. Comparing WT to S267C GlyR established what modifications in function occurred due to the mutation, while the addition of PMTS showed the effect of modulation of the receptor. We were able to compare these changes directly to ethanol effects on WT GlyR (Welsh et al., 2009) and saw many similarities indicating that PMTS effects on S267C receptors overall mimic ethanol effects on WT GlyR. These results have implications for the molecular mechanism of alcohol action on GlyR function.

4.2 Alcohol and anesthetic action

The GlyR has been extensively studied but the definitive site of alcohol and anesthetic binding and the molecular mechanism of action remains elusive. This study provides clarification on the location of the binding pocket and implicates an important role for residue 267. Jenkins et al. (2001) helped established the boundaries for the

binding cavity of another LGIC, the $GABA_AR$. Using three anesthetics, a common site of action on the receptor was determined, at the whole cell level. Three amino acids, including S270 that is analogous to S267 in the GlyR, played a role in defining the location of the binding pocket.

Single channel analysis results, presented in this dissertation, provide a descriptive mechanism of the changes incurred following the binding of an alcohol analog. S267C revealed an increase in burst duration due to increased time constants. Although a detailed mechanism of activation was not modeled in the absence and presence of PMTS, our data explains the enhanced potentiation of GlyR function observed at the whole cell level. Eggers and Berger (2004) found ethanol enhanced, in a dose-dependent manner, currents in native α1β GlyR in excised patches from rat hypoglossal motoneurons. Ethanol caused no change in conductance of the GlyR while increasing the numbers of open channels. A decreased glycinergic response rise-time and increased current decay time led the authors to the conclusion that ethanol's enhancing effect was through its increasing association (k_{on}) and decreasing dissociation (k_{off}) of glycine.

Currently, there is no crystal structure of the GlyR with an alcohol or anesthetic molecule bound due to the low-affinity binding of alcohol and the technical difficulties in crystallizing such a protein. However, the structure of LUSH, the *Drosphila* odorant binding protein that detects small alcohols, has been crystallized (Kruse et al., 2003). Structural data from LUSH can be extrapolated to predict where ethanol will bind on the GlyR since they share a common binding motif. The crystal structure indicated a single, water filled, cavity with room for one alcohol molecule. This is similar to the results ascertained through mutagenesis experiments on the GlyR (Lobo et al., 2004a; Lobo et al., 2008) encouraging the likelihood that the binding pockets are comparable.

While ethanol could possibly be causing an indirect effect on WT GlyR function, we know for certain that PMTS is directly binding at the cysteine 267 residue. At the single channel level, it is unlikely that ethanol would produce the same effects as PMTS bound at the putative alcohol binding site, if it was exclusively interacting with another protein site. This evidence supports the hypothesis that the S267 residue plays a role in the GlyR alcohol and anesthetic binding pocket. The results of this dissertation provide a new line of evidence that S267 is part of the alcohol binding site on the GlyR.

This research also adds evidence to the suggestion that proteins are the major site of alcohol and anesthetic action. While it is possible that PMTS could bind at an amino acid residue, while ethanol interacts with the lipid bilayer, it seems unlikely that these two differing modes of action would produce the same single channel alterations on GlyR function as observed. These two compounds produce similar effects suggesting they are both interacting with a defined binding site on the GlyR, and thus arguing against the lipid theory of alcohol and volatile anesthetic actions.

4.3 Future experiments

While the findings provided in this dissertation advance our understanding of the location of the putative alcohol and anesthetic binding pocket on the GlyR, it also generates more questions to be answered, some of which are described below.

1. The MTS reagent, PMTS, was selected for this study because its small size mimics alcohol. However, other MTS reagents of differing lengths should also be tested. In addition, other alcohols, such as propanol, should be evaluated as additional controls.

2. A higher concentration of PMTS (eg 10 mM) on WT GlyR should be tested to see if the enhancing trend we saw becomes a statistically significant effect.

3. The addition of PMTS covalently bound at S267C caused a change in conductance and an increase in burst duration. It would be interesting to add volume to the alcohol binding pocket using mutagenesis on WT GlyR by introducing a large amino acid at S267. Single channel experiments measuring the conductance and burst properties could be compared to the results of S267C GlyR in the presence of PMTS. This would answer the question of whether the changes caused by PMTS covalently bound at S267C can be mimicked by additional volume. Alternatively, the GABA S270 residue should be mutated to see if this conserved residue plays an important role in receptor conductance.

4. The decrease in S267C GlyR conductance could be the result of intra-subunit cysteine crosslinking, since disulfide bond formation can occur spontaneously. PMTS was pre-applied in our experiments with the unbound reagent washed off prior to applying glycine. PMTS application in the closed state of the receptor and binding at the putative binding pocket before glycine was applied might have prevented crosslinking from occurring. Applying PMTS and glycine in the open state to S267C would answer this question. It would be interesting to see if the conductance could change during a recording. First, glycine would be applied to the S267C GlyR resulting in a lower observed conductance followed by co-applying PMTS with glycine to see if the conductance increased. If there is no change in conductance upon PMTS application then a follow-up experiment using dithiothreitol, which reduces disulfide bonds that have formed, could be applied to S267C perfused with glycine. If there is a change in

conductance then crosslinking between cysteine residues is potentially occurring and responsible for the lower conductance observed.

5. We observed a significant decrease in single-channel conductance produced by the S267C mutation, and its restoration (to the WT level) by PMTS. Follow up work examining what role this plays in the structure and gating of the S267C GlyR would be intriguing. Additionally, a detailed kinetic model of S267C GlyR in the absence and presence of PMTS needs to be constructed. This model would be complex due to the incorporation of a primary subconductance state seen with S267C GlyR that is different then the main conductance in the presence of PMTS.

4.4 Summary

Ethanol and PMTS allosteric modulation of the GlyR does not mimic high concentrations of glycine. As shown in the data, the only significant change caused by both ethanol and PMTS is an increase in burst component lifetimes leading to longer burst durations. Also important are parameters of channel function that did not change in the presence of ethanol or PMTS, namely open-dwell times and most closed dwell times. This striking similarity leads us to believe that ethanol and PMTS are indeed binding at the same location. This study provided a descriptive mechanism of thiol binding to the alcohol binding site providing additional evidence to support the hypothesis that alcohol binds at S267 and that this residue is part of the binding pocket. Our work provides another step in the pursuit of the alcohol binding site since drugs designed to target this location could prove beneficial when treating alcoholism.

In conclusion, we found many similarities between the effects of PMTS covalently bound to the S267C residue in the α1 subunit and ethanol effects on WT GlyR. These data provide strong, albeit still indirect, supporting evidence that ethanol is exerting its enhancing effects on the glycine receptor via its interactions with at least amino acid residue 267 in the second transmembrane domain. Out data are consistent with the hypothesis that alcohols and anesthetics act in water-filled pockets found between transmembrane domains in the cys-loop family of receptors.

Bibliography

Aguayo LG and Pancetti FC. (1994) Ethanol modulation of the g-aminobutyric acid a- and glycine- activated Cl- current in cultured mouse neurons. J Pharmacol Exp Ther 270:61-69.

Aguayo LG, Tapia JC, and Pancetti FC. (1996) Potentiation of the glycine-activated Cl- current by ethanol in cultured mouse spinal neurons. J Pharmacol Exp Ther 279:1116-1122.

Ahrens J, Leuwer M, Stachura S, Krampfl K, Belelli D, Lambert JJ, and Haeseler G. (2008) A transmembrane residue influences the interaction of propofol with the strychnine-sensitive glycine alpha1 and alpha1beta receptor. Anesth Analg 107(6):1875-83.

Akk G, Bracamontes JR, Covey DF, Evers A, Dao T, and Steinbach JH (2004). Neuroactive steroids have multiple actions to potentiate GABAA receptors. J Physiol 558:59-74.

Antognini JF and Schwartz K. (1993) Exaggerated anesthetic requirements in the preferentially anesthetized brain. Anesthesiology 79:1244-1249.

Beato M, Groot-Kormelink PJ, Colquhoun D, and Sivilotti LG. (2002) Openings of the rat recombinant alpha 1 homomeric glycine receptor as a function of the number of agonist molecules bound. J Gen Physiol 119(5):443-466.

Beato M, Groot-Kormelink PJ, Colquhoun D, and Sivilotti LG. (2004) The activation mechanism of alpha1 homomeric glycine receptors. J Neurosci 24(4):895-906.

Beckstead M, Phelan R, and Mihic SJ 2001. Antagonism of inhalant and volatile anesthetic enhancement of glycine receptor function. J Biol Chem 6;276(27):24959-64.

Bertaccini EJ, Shapiro J, Brutlag DL, and Trudell JR. (2005) Homology modeling of a human glycine alpha 1 receptor reveals a plausible anesthetic binding site. J Chem Inf Model 45(1):128-35.

Betz H. (1991) Glycine receptors: heterogeneous and widespread in the mammalian brain. Trends Neurosci 14:458-461.

Betz H and Laube B. (2006) Glycine receptors: recent insights into their structural organization and functional diversity. J Neurochem 97(6):1600-1610.

Bowery NG and Smart TG. (2006) GABA and glycine as neurotransmitters: a brief history. Br. J. Pharmacol 147 Suppl 1, S109-S119.

Brejc K, van Dijk WJ, Klaassen RV, Schuurmans M, van Der Oost J, Smit AB, and Sixma TK. (2001) Crystal structure of an ACh-binding protein reveals the ligand-binding domain of nicotinic receptors. Nature 411:269-276.

Burzomato V, Beato M, Groot-Kormelink PJ, Colquhoun D, and Sivilotti LG (2004) Single channel behavior of heteromeric alpha1beta glycine receptors: an attempt to detect a conformational change before the channel opens. J Neurosci 24: 10924-10940.

Celentano JJ, Gibbs TT, and Farb DH. (1988) Ethanol potentiates GABA and glycine induced currents in chick spinal cord neurons. Brain Res. 455:377-380.

Colquhoun D and Sivilotti LG. (2004) Function and structure in glycine receptors and some of their relatives. Trends in Neurosciences 27: 337-344.

Colquhoun D and Sigworth FJ. (1995) Fitting and Statistical Analysis of Single-Channel Records. In: Single-channel Recording (Sakmann B, Neher E, eds), pp 483-587. New York: Plenum Press.

Crawford DK, Trudell JR, Bertaccini EJ, Li K, Davies DL and Alkana RL. (2007) Evidence that ethanol acts on a target in Loop 2 of the extracellular domain of alpha1 glycine receptors. J Neurochem 102(6):2097-2109.

Dime DS. (1997) Methanethiosulfonate Reagents: Application to the Study of Protein Topology and Ion Channels, Toronto Research Chemicals Reference Sheet.

Downie DL, Hall AC, Lieb WR, and Franks NP. (1996) Effects of inhalational general anaesthetics on native glycine receptors in rat medullary neurones and recombinant glycine receptors in Xenopus oocytes. Br J Pharmacol 118:493-502.

Dupre ML, Broyles JM, and Mihic SJ (2007) Effects of a mutation in the TM2-TM3 linker region of the glycine receptor alpha1 subunit on gating and allosteric modulation. Brain Res 1152:1-9.

Eger EI, Saidman LJ, and Brandstater B. (1965) Minimum alveolar anesthetic concentration: a standard of anesthetic potency. Anesthesiology 26 (6): 756–63.

Eggers ED and Berger AJ. (2004)Mechanisms for the modulation of native glycine receptor channels by ethanol.J Neurophysiol 91(6):2685-95.

Findlay GS, Wick MJ, Mascia MP, Wallace D, Miller GW, Harris RA, and Blednov YA. (2002) Transgenic expression of a mutant glycine receptor decreases alcohol sensitivity of mice. J Pharmacol Exp Ther 300:526-534.

Findlay GS, Phelan R, Roberts MT, Homanics GE, Bergeson SE, Lopreato GF, Mihic SJ, Blednov YA, and Harris RA. (2003) Glycine receptor knock-in mice and hyperekplexia-like phenotypes: comparisons with the null mutant. J Neurosci 23:8051-8059.

Franks NP and Lieb WR. (1984) Do general anaesthetics act by competitive binding to specific receptors? Nature 310(5978): 599-601.

Freshney RI. (2000) Culture of animal cells: a manual of basic technique. New York: Wiley.

Jung S, Akabas MH, and Harris RA. (2005) Functional and structural analysis of the GABAA receptor alpha 1 subunit during channel gating and alcohol modulation. J Biol Chem 280(1):308-316.

Grasshoff C and Antkowiak B. (2006) Effects of isoflurane and enflurane on GABAA and glycine receptors contribute equally to depressant actions on spinal ventral horn neurones in rats Br J Anaesth 97(5):687-94.

Griffon N, Büttner C, Nicke A, Kuhse J, Schmalzing G, and Betz H. (1999). Molecular determinants of glycine receptor subunit assembly. EMBO J. 18(17):4711-4721.

Groot-Kormelink PJ, Beato M, Finotti C, Harvey RJ, and Sivilotti LG (2002) Achieving optimal expression for single channel recording: a plasmid ratio approach to the expression of alpha 1 glycine receptors in HEK293 cells. J Neurosci Methods 113: 207-214.

Grudzinska J, Schemm R, Haeger S, Nicke A, Schmalzing G, Betz H, and Laube B. (2005). The β subunit determines the ligand binding properties of synaptic glycine receptors. Neuron 45: 727-739.

Hamill OP, Marty A, Neher E, Sakmann B, and Sigworth FJ (1981) Improved patch-clamp techniques for high-resolution current recording from cells and cell-free membrane patches. Pflugers Arch 391:85-100.

Hamill OP, Bormann J, and Sakmann B (1983) Activation of multiple-conductance state chloride channels in spinal neurones by glycine and GABA. Nature 305(5937):805-808.

Hsiao B, Mihalak KB, Magleby KL, Luetje CW. (2008) Zinc potentiates neuronal nicotinic receptors by increasing burst duration. J Neurophysiol 99(2):999-1007.

Ivanova E, Muller U, and Wassle H. (2006) Characterization of the glycinergic input to bipolar cells of the mouse retina. Eur J Neurosci 23:350-364.

Karlin A and Akabas MH. (1998) Substituted-cysteine accessibility method. Methods Enzymol 293:123-145.

Keramidas A and Harrison NL. (2008) Agonist-dependent single channel current and gating in alpha4beta2delta and alpha1beta2gamma2S GABAA receptors. J Gen Physiol 131(2):163-81.

Lape R, Colquhoun D, and Sivilotti LG (2008). On the nature of partial agonism in the nicotinic receptor superfamily Nature 454(7205):722-727.

Laube B, Kuhse J, Rundström N, Kirsch J, Schmieden V, and Betz H. (1995) Modulation by zinc ions of native rat and recombinant human inhibitory glycine receptors. J Physiol 483:613-619.

Laube B, Kuhse J, and Betz H. (2000) Kinetic and mutational analysis of Zn2+ modulation of recombinant human inhibitory glycine receptors. J Physiol 522(2):215-230.

Laube B, Maksay G, Schemm R, and Betz H. (2002) Modulation of glycine receptor function: a novel approach for therapeutic intervention at inhibitory synapses? Trends in Pharmacological Sciences 23: 519-527.

Lema GM and Auerbach A. (2006) Modes and models of GABA(A) receptor gating. J Physiol 572(Pt 1):183-200.

Lynch JW. (2004) Molecular structure and function of the glycine receptor chloride channel. Physiol Rev 84:1051-1095.

Legendre P. (2001) The glycinergic inhibitory synapse. Cell Mol Life Sci 58:760-793.

Lobo IA, Mascia MP, Trudell JR, and Harris RA. (2004a) Channel gating of the glycine receptor changes accessibility to residues implicated in receptor potentiation by alcohols and anesthetics. J Biol Chem 279(32):33919-33927.

Lobo IA, Trudell JR, and Harris RA. (2004b) Cross-linking of glycine receptor transmembrane segments two and three alters coupling of ligand binding with channel opening. J Neurochem 90(4):962-969.

Lobo IA, Trudell JR, and Harris RA. (2006) Accessibility to residues in transmembrane segment four of the glycine receptor. Neuropharmacology 50(2):174-181.

Lobo IA, Harris RA, and Trudell JR. (2008) Cross-linking of sites involved with alcohol action between transmembrane segments 1 and 3 of the glycine receptor following activation. J Neurochem 104(6):1649-1662.

Maas C, Tagnaouti N, Loebrich S, Behrend B, Lappe-Siefke C, and Kneussel M. (2006) Neuronal cotransport of glycine receptor and the scaffold protein gephyrin. J Cell Biol 172: 441-451.

Mascia MP, Mihic SJ, Valenzuela CF, Schofield PR, and Harris RA. (1996) A single amino acid determines differences in ethanol actions on strychnine-sensitive glycine receptors. Mol Pharmacol 50:402-406.

Mascia MP, Trudell JR, and Harris RA. (2000) Specific binding sites for alcohols and anesthetics on ligand-gated ion channels. Proc Natl Acad Sci 97(16):9305-9310.

McCracken LM, Trudell JR, Goldstein BE, Harris RA, Mihic SJ. Zinc enhances ethanol modulation of the α1 glycine receptor. *Submitted* Neuropharmacology.

Meyer H. (1899) Zur Theorie der Alkoholnarkose. Arch Exp Pathol Pharmakol 42:109-118.

Mihic SJ, Ye Q, Wick MJ, Koltchine VV, Krasowski MD, Finn SE, Mascia MP, Valenzuela CF, Hanson KK, Greenblatt EP, Harris RA, and Harrison NL. (1997) Sites of alcohol and volatile anaesthetic action on GABA(A) and glycine receptors. Nature 389(6649): 385-389.

Miller PS, Da Silva HM, and Smart TG. (2005) Molecular basis for zinc potentiation at strychnine-sensitive glycine receptors. J Biol Chem 280(45):37877-37884.

Miller R. (2005) Miller's Anesthesia. New York: Elsevier/Churchill Livingstone.

Miyazawa A, Fujiyoshi Y, and Unwin N. (2003) Structure and gating mechanism of the acetylcholine receptor pore. Nature 423(6943):949-955.

Molander A and Söderpalm B. (2005a). Accumbal strychnine-sensitive glycine receptors: an access point for ethanol to the brain reward system. Alcohol Clin Exp Res 29(1):27-37.

Molander A and Söderpalm B. (2005b). Glycine receptors regulate dopamine release in the rat nucleus accumbens. Alcohol Clin Exp Res 29(1):17-26.

Molander A, Löf E, Stomberg R, Ericson M, and Söderpalm B. (2005) Involvement of accumbal glycine receptors in the regulation of voluntary ethanol intake in the rat. Alcohol Clin Exp Res 29(1):38-45.

Neher E and Sakmann B. (1976) Single-channel currents recorded from membrane of denervated frog muscle fibres. Nature 260(5554):799-802.

Overton E. (1901) Studien über die Narkose, zugleich ein Beitrag zur allgemeinen Pharmakologie. Jena: Verlag von Gustav Fischer.

Peoples RW, Li C, and Weight FF. (1996) Lipid vs protein theories of alcohol action in the nervous system. Annu Rev Pharmacol Toxicol 36:185-201.

Pless SA and Lynch JW. (2009) Ligand-specific conformational changes in the alpha 1 glycine receptor ligand-binding domain. J Biol Chem 284(23):15847-15856.

Qin, F, Auerbach A, and F Sachs. (1996) Estimating single-channel kinetic parameters from idealized patch clamp data containing missed events. Biophysical Journal 70:264-280.

Qin F, Auerbach A, and F Sachs. (1997) Maximum likelihood estimation of aggregated Markov processes. Proceedings of the Royal Society B 264:375-383.

Qin F, Auerbach A, and Sachs F. (2000a) A direct optimization approach to hidden Markov modeling for single channel kinetics. Biophys J 79:1915-1927.

Qin F, Auerbach A, and Sachs F. (2000b) Hidden Markov modeling for single channel kinetics with filtering and correlated noise. Biophys J 79:1928-1944.

Qin F. (2004) Restoration of single-channel currents using the segmental k-means method based on hidden Markov modeling. Biophys 86(3):1488-1501

Quinlan JJ, Ferguson C, Jester K, Firestone LL, and Homanics GE. (2002) Mice with glycine receptor subunit mutations are both sensitive and resistant to volatile anesthetics. Anesth Analg 95:578-582.

Roberts MT, Phelan R, Erlichman BS, Pillai RN, Ma L, Lopreato GF, and Mihic SJ. (2006) Occupancy of a single anesthetic binding pocket is sufficient to enhance glycine receptor function. J Biol Chem 281(6):3305-3311.

Sine S and Engel A. (2006) Recent advances in Cys-loop receptor structure and function. Nature 440 (7083):448–55.

Tang MX, Redemann CT, and Szoka FC, Jr. (1996) In vitro gene delivery by degraded polyamidoamine dendrimers. Bioconjug Chem 7: 703-714.

Tapia JC, Aguilar LF, Sotomayor CP, and Aguayo LG. (1998) Ethanol affects the function of a neurotransmitter receptor protein without altering the membrane lipid phase. Eur J Pharmacol 354: 239-244.

Ueno S, Lin A, Nikolaeva N, Trudell JR, Mihic SJ, Harris RA and Harrison NL. (2000) Tryptophan scanning mutagenesis in TM2 of the GABAA receptor α subunit: effects on channel gating and regulation by ethanol. Br J Pharmacol 131:296-302.

Unwin N. (2005) Refined structure of the nicotinic acetylcholine receptor at 4A resolution. J Mol Biol 346(4):967-989.

Urban BW and Bleckwenn M. (2002) Concepts and correlations relevant to general anaesthesia. Br J Anaesth 89: 3-16.

Welsh BT, Goldstein BE, and Mihic SJ. (2009) Single-channel analysis of ethanol enhancement of glycine receptor function. JPET 330:198-205.

Wick MJ, Mihic SJ, Ueno S, Mascia MP, Trudell JR, Brozowski SJ, Ye Q, Harrison NL, and Harris RA. (1998) Mutations of gamma-aminobutyric acid and glycine receptors change alcohol cutoff: evidence for an alcohol receptor? Proc Natl Acad Sci U S A 95(11):6504-6509.

Xu M and Akabas MH. (1993) Amino acids lining the channel of the gamma-aminobutyric acid type A receptor identified by cysteine substitution. J Biol Chem 268(29):21505-21508.

Williams KL, Ferko AP, Barbieri EJ, and Di Gregorio GJ. (1995) Glycine enhances the central depressant properties of ethanol in mice. Pharmacol. Biochem. Behav 50:199-205.

World health organization website http://www.who.int/en/ world health organization

Ye Q, Koltchine VV, Mihic SJ, Mascia MP, Wick MJ, Finn SE, Harrison NL, and Harris RA. (1998) Enhancement of glycine receptor function by ethanol is inversely correlated with molecular volume at position alpha267. J Biol Chem. 273(6):3314-3319.

Ye JH, Tao L, Ren J, Schaefer R, Krnjevic K, Liu PL, Schiller DA, and McArdle JJ. (2001) Ethanol potentiation of glycine-induced responses in dissociated neurons of rat ventral tegmental area. J Pharmacol Exp Ther 296:77-83.

Yevenes GE, Moraga-Cid G, Peoples RW, Schmalzing G, and Aguayo LG. (2008) A selective G betagamma-linked intracellular mechanism for modulation of a ligand-gated ion channel by ethanol. Proc Natl Acad Sci U S A 105(51):20523-20528.

Zhang Y, Laster MJ, Hara K, Harris RA, Eger EI, Stabernack CR, and Sonner JM. (2003) Glycine receptors mediate part of the immobility produced by inhaled anesthetics. Anesth. Analg 96: 97-101.

Vita

Beth Erlichman Goldstein was born in Frederick, Maryland to Martin and Marianne Erlichman on December 9th 1979. She has an older sister Janelle Erlichman Diamond. She attended the University of Maryland, College Park from 1997 to 2001. She was selected for the life science scholars program and majored in Neurobiology & Physiology. After a post-baccalaureate year working at the National Institutes of Health, Beth moved to Austin to attend The University of Texas. As a graduate student in the Cellular and Molecular Biology Program she met her future husband, Glenn Goldstein, and they were married October 6, 2007. Beth's successful career in research has led to numerous published papers including a recent first author submission on her dissertation project. She was a teaching assistant for Dr. Adron Harris' Biology of Addiction class for two semesters. She will be awarded her PhD in August 2009 and currently resides with her husband and black lab, Murphy, in Austin.

Permanent address: 3411 Gable Drive, Austin, TX 78759

This dissertation was typed by Beth Erlichman Goldstein.